

# A review of globally available data sources for modelling the Water-Energy-Food Nexus

Jack W. Lodge<sup>\*</sup>, Andrew P. Dansie, Fiona Johnson

Water Research Centre, School of Civil and Environmental Engineering, UNSW, Sydney, Australia

## ARTICLE INFO

**Keywords:**  
Water-energy-food nexus  
Global data  
Remote sensing  
Reanalysis

## ABSTRACT

The Water-Energy-Food Nexus (WEFN) is gaining attention as an important approach to manage resources more holistically. Data availability, however, is a crucial barrier to WEFN implementation globally. To assist modellers and practitioners in navigating this barrier, 'data hierarchies' were created, based on a comprehensive review of openly globally available data in water, energy, and food sectors. Global data sources considered include Satellite Remote Sensing (RS), Reanalysis, Global Observation Networks and Land Surface Models. The data hierarchies detail what data are suitable for modelling water, energy, and food availability globally. Furthermore, the review has highlighted which variables are not well monitored by global data sources, and for the first time has discussed global data sources' interactions in the WEFN. The findings from the review and the associated data interactions have been used to recommend priority areas from a WEFN perspective for improving global data availability, and include streamflow, wind speed, and hydropower data.

## 1. Introduction

The Water-Energy-Food Nexus (WEFN) promotes coordination and collaboration across its constituent sectors (FAO, 2014), to identify trade-offs, synergies, and the most beneficial policies across all sectors (Bazilian et al., 2011). This builds on the integrated water resources management (IWRM) approach, but the WEFN instead considers the water, energy, and food sectors with equal importance (Wicaksono et al., 2017; Bach et al., 2012). The WEFN approach is critical to achieving the UN's Sustainable Development Goals (SDGs) relating to water, energy, and food (Pahl-Wostl, 2019) as well as the interlinkages between all SDGs (Scharlemann et al., 2020; Requejo-Castro et al., 2020). The nexus is thus an important research area globally for future sustainable development.

To implement the WEFN, science needs to identify the key trade-offs and synergies which exist between sectors, which is challenging, especially when considering data availability and compatibility across sectors. The availability of data is regarded as one of the major challenges in implementing the WEFN (Vinca et al., 2021b; Kaddoura and El Khatib, 2017; Liu et al., 2017). The aim of this paper is to assist WEFN practitioners in navigating this challenge around data availability by 1) assessing globally available data sources in each of the water, energy, and food sectors and 2) developing a hierarchical decision-support tool

to select data suitable for nexus-based modelling at national-, regional-, or basin-scales. National, regional-, and basin-scales are the focus of the paper because the WEFN is generally implemented at these spatial scales. Thus, the focus is on globally-available data rather than data suitable for global-scale analyses.

Globally-available data (hereafter global data), for example Satellite Remote Sensing (RS), have been used widely in water, energy, and/or food nexus assessments (Al Zayed and Elagib, 2017; Basheer et al., 2021; Alam et al., 2019) and for understanding water and energy cycles and budgets (L'Ecuyer et al., 2015; Rodell et al., 2015). Global data sources thus have a valuable role in WEFN analysis and understanding resource availability. However, the large number of data products and associated assessments of these data products for individual water, energy, and food sectors make it difficult to evaluate them for the purposes of WEFN modelling. There has to date been no attempt to review and synthesize all globally available data for water, energy, and food sectors, nor to assess if there are variables which do not have any global data available. This paper addresses this gap.

While comprehensive global reviews have been completed for some variables, e.g. precipitation (Sun et al., 2018), reviews of other variables are limited, either being outdated and/or not comprehensive. Solar energy estimation using global data sources has not been comprehensively reviewed since 2003 (Hammer et al., 2003), and even then, only

\* Corresponding author.

E-mail address: [jack.lodge@unsw.edu.au](mailto:jack.lodge@unsw.edu.au) (J.W. Lodge).

RS was considered. The use of global data for understanding groundwater resources has not been comprehensively reviewed since 2007 (Jha et al., 2007; Becker, 2006). Reviews since then have focussed on one aspect of groundwater, e.g., groundwater potential mapping, considering various auxiliary data (Díaz-Alcaide and Martínez-Santos, 2019), but they have not considered all groundwater attributes that can be estimated by RS. Hydropower does not have any comprehensive review of the use of RS or other global data. Furthermore, some reviews are in sub-discipline literature and therefore may not be accessible to all WEFN practitioners e.g. an irrigation focus for evapotranspiration (ET) products (Massari et al., 2021). Thus, it can be difficult for practitioners working in the WEFN to find global data sources when local data are unavailable.

This paper aims to address the gaps in knowledge of open, global data that are suitable for modelling and implementing the WEFN. Thus, data from global ground observation databases, Land Surface Models (LSMs), reanalysis, and RS are reviewed. Literature was reviewed on each water, energy, and food sector, to summarise data availability, resolution, and the uncertainties of these data types and sources. This paper provides guidance for the rapid assessment of water, energy, and food data availability as the first step in the design and implementation of WEFN at regional, national, and transboundary levels.

## 2. Globally available data for the WEFN

There are four main types of global datasets discussed here: RS, reanalysis, LSMs, and global ground observation databases. The focus here is on primary data sources, so although there are other datasets available from, for example, process-based numerical models and machine learning models, these have generally not been included to limit the scope of the review. Where these outputs have promise in terms of addressing important gaps for the WEFN, readers are directed to pertinent resources in the relevant sub-section. In this section, an overview of the datasets and general advantages and limitations of each are provided. Benefits at global scales may not always apply for specific locations, and local case studies may still be required to understand what datasets are best for any given location.

Throughout this review, “variable” has been used to describe each data type or source, i.e., soil moisture, wind energy, solar energy, and crop area, are all referred to as variables. Some of the “variables” could alternatively be referred to as processes, parameters, forcings or predictors, particularly in a modelling context. “Variables” has been chosen for consistency. Furthermore, when discussing WEFN modelling, reference is to both conceptual and numerical modelling, where the former is framework for representing the WEFN interactions and systems and the latter represents a collection of mathematical equations to simulate one or more variables.

### 2.1. Remote sensing

RS provides information about an area, object, or phenomenon without contact with said area, object, or phenomenon (Lillesand et al., 2015). This can include data collected by ground based RS, aircraft, unmanned aerial vehicles, or satellites. Satellite RS is the primary focus of RS discussed in this paper. There are two types of RS data available: passive: which is information attained by sensors of the Earth's naturally emitted energy; and active: where energy is transmitted by a sensor to elicit information of interest (Lillesand et al., 2015). In either case, the variables of interest are not directly measured by RS, and numerical models are used to estimate them from the direct measurements.

Optical RS imagery has the advantage of being available at relatively high spatial resolution (Musa et al., 2015), but cloudy conditions present substantial barriers if data are required at fine temporal resolution. Radar and microwave RS can penetrate clouds and can also measure Earth systems at night (Musa et al., 2015).

### 2.2. Reanalysis

Reanalysis datasets use data assimilation to constrain earth system models with observation data to generate gridded simulations across the earth's surface and vertically through the atmosphere and oceans (Bosilovich et al., 2008). The reanalysis models considered here for the variables of interest are routinely updated to present day (with a small delay for collection and processing of information). Spatial resolution is lower than many RS products, but temporal coverage is usually much longer. Reanalyses estimate almost all the variables discussed in this review. However due to their relatively coarse resolution, reanalysis data do not provide useful estimates for numerical modelling of the all WEFN variables discussed here at the spatial scales of interest.

### 2.3. Land surface models

LSMs are numerical models which simulate coupled land surface – atmosphere processes, including carbon, energy, and water (Bonan, 1996). When included as part of a General Circulation Model (GCM) or Earth System Model with potential future radiative forcings, LSMs can also be used to project future changes of the Earth system (Fisher and Koven, 2020), including changes in surface hydrology, vegetation, and crops (Fisher and Koven, 2020), all relevant to the WEFN.

### 2.4. Global openly available observation networks and gridded products

Global observation networks, based on in situ measurements, are available for some important variables for modelling the WEFN. One of the limitations of these networks is their lack of spatial and temporal homogeneity, because the ground observation network density has been variable in time and space. Global observation networks frequently lack data in remote regions and over large bodies of water, including lakes. Thus, gridded products developed from gauged data have varying bias and uncertainty according to gauge density. Furthermore, although the overall product may cover a long period, missing data at individual sites can be a substantial problem and the maximum temporal coverage is usually only available for a subset of the sites.

## 3. Water, energy, food data review

The datasets reviewed cover variables required for understanding WEFN availability. The most widely used data in the literature for each sector are covered. Secondary data used in equations for estimating variables are not considered, e.g., the inputs for the Penman Monteith estimates of evapotranspiration have been omitted to limit the scope of the review. Ground and aerial based RS products have also been omitted, as these are not globally available. Temporal resolution is an important consideration when selecting datasets. Monthly time steps are commonly used in WEFN studies (Bakhshianlamouki et al., 2020; Sušnik et al., 2021; Yang et al., 2016) and capture seasonality. However finer temporal resolutions would be necessary if the WEFN modelling is designed to understand extreme event impacts, system planning, or non-linear interactions among variables. Furthermore, whilst monthly is considered sufficient for capturing seasonality, coarse temporal resolution input data producing monthly values could result in omission of important events within that month for certain variables causing uncertainties in datasets. An example of this is river discharge; although a satellite overpass such as SWOT may fulfil the monthly resolution ability (21 days (NASA, 2020)), collecting data for one event in the month is unlikely to be representative of flow for the whole month in many locations. Thus, consideration of variable temporal fluctuations is important when considering whether a monthly observation of a given product is suitable.

**Table 1**

Open, globally available data used for water modelling.

Water Information	Data Required	Data Available
Precipitation	Precipitation	Reanalysis Remote Sensing Gridded Gauge Products
Evapotranspiration	Evapotranspiration	Merged Reanalysis or Ground Observations with Remote Sensing
Streamflow	Streamflow	Remote Sensing and/or Reanalysis used in Global Model
Soil Moisture	Soil Moisture	Remote Sensing LSM
Groundwater	Subsidence Vegetation Groundwater Potential	Reanalysis Remote Sensing Remote Sensing
Lake Variation	Depletion Estimates Level Area Storage Change	Remote Sensing Remote Sensing Remote Sensing Remote Sensing

### 3.1. Water

Although a WEFN framework considers all sectors equally, water does have a special role in the nexus, as in many applications water cannot be replaced with alternative resources (Cansino-Loeza and Ponce-Ortega, 2021; Zhang et al., 2018; World Economic Forum, 2011). There are a wide range of global openly available data and tools for hydrological modelling and understanding, covering most hydrological processes (Table 1).

#### 3.1.1. Precipitation

Precipitation is the major driver of surface water availability and variability in the hydrological cycle and thus, precipitation data are imperative for estimating runoff. Global precipitation data can be collected from global databases of ground observations, satellite RS, and reanalysis (Fig. 1). Although precipitation data are available worldwide from ground observations, often the density of stations is too low to provide accurate distributions of precipitation over larger areas (Kidd and Huffman, 2011). This affects water balance in hydrological models,

and further impacts the irrigation requirement estimates for the food sector. For more extensive details of existing precipitation products reference should be made to Sun et al. (2018).

Different precipitation data are advised in the data hierarchy with the choice of product based on gauge network density, temperature/climate, and timespan of data required (Fig. 1). Reliability of gridded surface gauge data depends on the availability of gauges in the region and quality of gauged data, reliability is lower where station density is lower (Rudolf et al., 1994; Schamm et al., 2014), and the published temporal coverage of a product does not always represent temporal coverage of data in the area of concern. Thus, where station density is low or temporal coverage is short, gridded surface gauge products should not be used.

Depending on climate, different datasets have varying accuracy in representing rainfall. At higher latitudes ( $>40^\circ$ ), reanalysis products are recommended because RS products are often unavailable at high latitudes (Tang et al., 2020; Beck et al., 2017). Where ground is frozen, or snow cover is present, some RS products do not estimate rainfall well, and reanalysis sometimes performs better (Massari et al., 2017). In

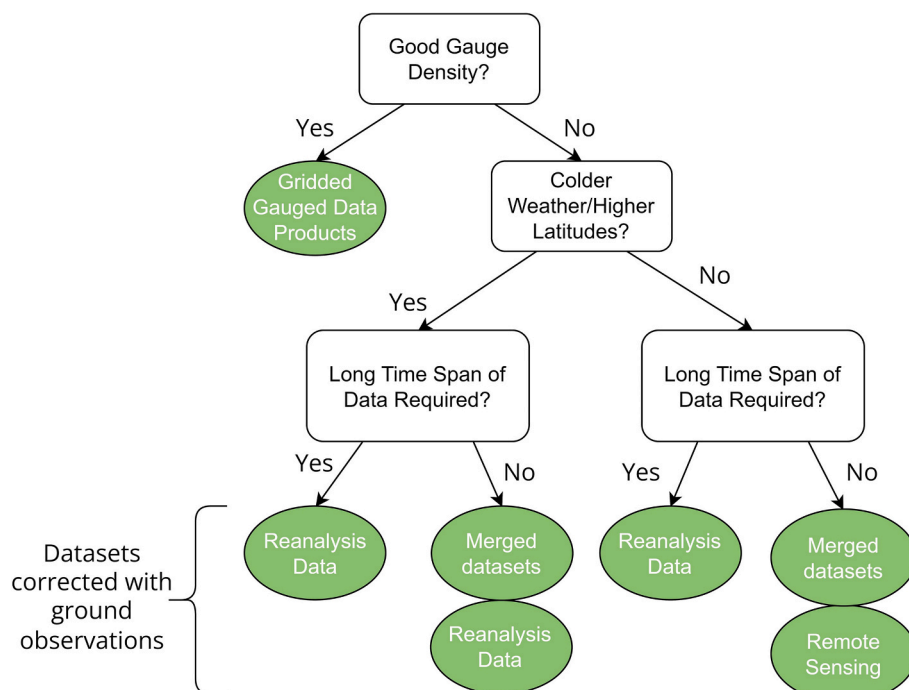


**Fig. 1.** Hierarchy of available global precipitation data sources. Longer time spans of data are indicative of data required for over 40 years. The adequacy of gauge density is dependent on area of study, reference should be made to Section 2.4.2 of WMO (2008), for more information.

**Table 2**

Different global precipitation data types and examples of datasets available. Spatial resolution, temporal resolution, temporal coverage, \*: gauge corrected, (\*): Both gauge corrected and uncorrected available. Adapted from Beck et al. (2019a).

Data Type	Dataset/ Satellite Mission	Spatial Resolution	Temporal Resolution	Spatial Coverage	Temporal Coverage	Source
Global Gauged Gridded	Climate Prediction Center (CPC)	0.5°	Daily	Global	1948–2018	(Xie et al., 2010)
	Global Precipitation Climatology Centre (GPCC)	0.25°/1°	Monthly/ Daily	Global	1891–2018	(Rudolf et al., 2010)
	University of Delaware (UDEL)	0.5°	Monthly	Global	1900–2017	(Matsuura and Willmott, 2018)
Remote Sensing	CMORPH	0.07°	0.5 Hour	60°N–60°S	1998–Present	(Xie et al., 2019)
	GSMaP (*)	0.1°	Hourly	60°N–60°S	2000–Present	(Okamoto et al., 2005)
	IMERG (*)	0.1°	0.5 Hour	Global	2000–Present	(Huffman et al., 2015) (Huffman et al., 2020)
Reanalysis	PERSIANN (*)	0.25°	Hourly	60°N–60°S	2000–Present	(Sorooshian et al., 2014)
	TRMM (*)	0.25°	3 Hourly	50°N–50°S	1998–Present	(Huffman et al., 2010)
	ERA5	0.28°	Hourly	Global	1950–Present	(Hersbach et al., 2020)
Merged Data	JRA-55	0.56°	3-Hourly	Global	1959–Present	(Kobayashi et al., 2015)
	MERRA-2 *	0.5°	Hourly	Global	1979–Present	(Gelaro et al., 2017)
	The Climate Hazards Group InfraRed Precipitation with Station Data (CHIRPS) *	0.05°	Daily	50°N–50°S	1981–Present	(Funk et al., 2015)
	Global Precipitation Climatology Project (GPCP) *	1°	Daily	Global	1996–2015	(Adler et al., 2018)
	Multi-Source Weighted-Ensemble Precipitation, Version 2 (MSWEP V2) *	0.1°	3-Hourly	Global	1979–Present	(Beck et al., 2019b)
	PERSIANN CCS-CDR	0.04°	3-Hourly	60°N–60°S	1983–Present	(Sadeghi et al., 2021)
	PERSIANN-CDR	0.25°	Daily	60°N–60°S	1983–Present	(Ashouri et al., 2015)

summer months in tropical wet climates, RS often performs better than reanalysis, which does not represent localised convective storms well (Beck et al., 2019a; Hu et al., 2016; Massari et al., 2017; Beck et al., 2017). Several RS sensors are used for rainfall data, including Passive Microwave (PM), Active Microwave (AM), and infrared (IR) (Michaeldes et al., 2009). PM spatial and temporal sampling is often too low for localised events, whilst neither PM nor IR capture warm orographic rainfall over complex terrain well (Derin and Yilmaz, 2014). A combination of both passive and active sensors are beneficial for estimating precipitation (Levizzani and Cattani, 2019). Temperate regions are usually better represented than arid regions (Xiang et al., 2021). Merged products, combining RS, reanalysis, and correcting with gauged data, typically represent rainfall best (Xiang et al., 2021; Beck et al., 2017; Beck et al., 2019a), and are thus recommended first.

There are major challenges in collecting snow depth and converting it to snow water equivalent (SWE) data using RS, especially in mountainous areas, although snow cover extent is better understood (Lettmaier et al., 2015; Skofronick-Jackson et al., 2015). There are also challenges in understanding performance of precipitation products in many snow covered regions, due to lack of in situ gauges (Palmer et al., 2017; Wrzesien et al., 2019). SWE is of particular importance for WEFN analyses in mountainous catchments where snowmelt dominates annual and seasonal water flows, providing water for hydropower and crops. Optical sensors can estimate snow cover area, whilst passive and active microwave are capable of estimating SWE, although PM's spatial resolution limit its ability in mountainous areas (Largeron et al., 2020). Several reanalysis datasets can also be used to monitor snow water depth, including MERRA, ERA, and GLDAS with large uncertainties (Wrzesien et al., 2019). In the European Alps, CHIRPS, a merged precipitation dataset, had reasonable skill in modelling snow (Weber et al., 2021). Treichler and Kääb (2017), detected snow depth with ICESat and high accuracy DEMs. However ICESat's revisit time (91-days), means it is unsuitable for monthly analysis. Lievens et al. (2019), showed that Sentinel-1 SAR could capture inter-annual variations and spatial variability of snow in mountain ranges in the northern hemisphere. A more comprehensive review on the current state of snow depth can be found in Largeron et al. (2020).

Temporal coverage of precipitation data varies widely (Table 2). If over 40 years of data are required, e.g. for climate scenarios, reanalysis is better (Sun et al., 2018), because merged and RS datasets are often only available for 20–40 years (Beck et al., 2019b). Whilst 30 to 40 years

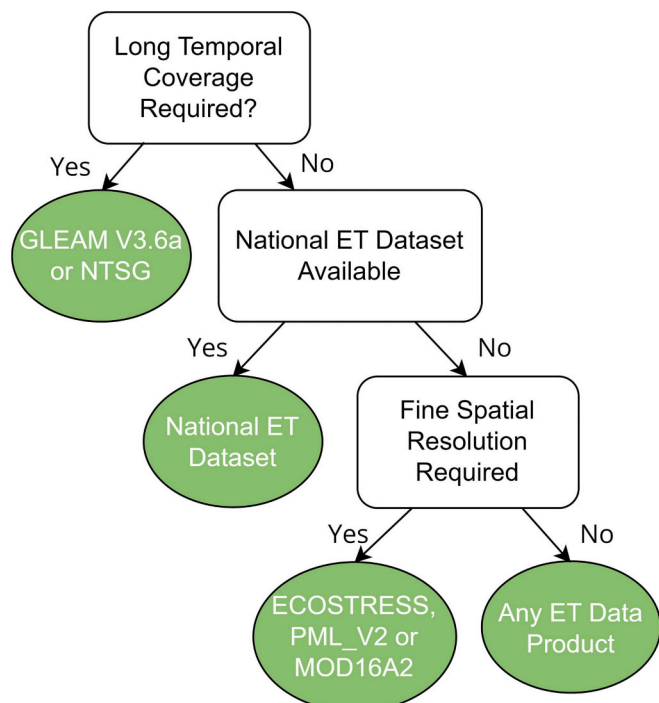


**Fig. 2.** Evapotranspiration data hierarchy. The products mentioned here are those which contain ET data which can be directly downloaded.

of data are adequate for analysing climatological means and seasonal variability, longer time series are generally required to understand the impacts of interannual variability, including droughts and pluvial extremes. However in many locations, even century-long observational records do not capture the full spectrum of such variability, particularly when non-stationarity is exacerbated by anthropogenic climate change (Milly et al., 2008). Resilient WEFN policies will likely require testing with climate scenarios and/or paleoclimate-informed stochastic simulations.

The WEFN is often analysed using a monthly temporal resolution and at this resolution, most precipitation products have adequate skill. However, if the impacts of short duration extreme events are important

**Table 3**

Openly available ET data products available at the global level.

Data Type	Dataset/ Satellite Mission	Spatial Resolution	Temporal Resolution	Spatial Coverage	Temporal Coverage	Source
Merged RS and GMAO	MOD16A2	500 m	8-Day	Global	2001- present	(Mu et al., 2011)
Merged RS and GLDAS	PML V2	500 m	8-Day	60°S-90°N	2002-2019	(Zhang et al., 2019)
Merged RS with GDAS	SSEBop	10 km	10-Day	Global	2003-2014	(Senay et al., 2020)
Merged RS with Reanalysis	GLEAM V3.6a	0.25°	Daily	Global	1980- present	(Martens et al., 2017)
Merged RS with Reanalysis	SEBS	5 km	Daily and monthly	Global	2000-2017	(Chen et al., 2021)
Merged RS, Reanalysis, and Flux Towers	NTSG	1°	Daily	62°S-90°N	1983-2013	(Zhang et al., 2010)
Remote Sensing	GLEAM V3.6b	0.25°	Daily	Global	2003- present	(Martens et al., 2017)
Remote Sensing	ECOSTRESS PT-JPL	70 m	Daily	Global	2018-present	(Fisher et al., 2020)

then products should be chosen accordingly (Table 2). For example, the cross sectoral impacts of short duration, extreme floods on food supply and transport, particularly in the context of spatially or temporally compound events is an active area of research.

### 3.1.2. Evapotranspiration

ET data are imperative in deriving irrigation requirements (Brouwer and Heibloem, 1985) and catchment losses. Thus, ET represents a key water-food interaction in the WEFN. ET is physically driven by solar radiation, wind speed, humidity deficit, temperature, soil moisture, crop type, and crop stage (Brouwer and Heibloem, 1985). ET is difficult to measure directly and there are many methods for estimating ET, including empirical, energy budget, deterministic, and vegetation index (VI) methods, which have varying levels of complexity and data requirements (McMahon et al., 2013). As a result, ET differs from the other variables reviewed here, with algorithms using a variety of data sources, combining indices and products (Zhang et al., 2016a). ET has high spatial variability, making in situ data collection at adequate spatial resolution difficult (Liu et al., 2010). This section gives a brief overview of ET numerical models that directly provide globally available ET estimates.

The driving factors to select ET data are temporal coverage, spatial resolution, and availability of in-country datasets (Fig. 2). If over 20 years of data are required for analysis in the WEFN, reanalysis-merged datasets, like GLEAM V3.6a or NTSG are available from 1980 (Table 3). If available, national ET datasets are advised because of their finer spatiotemporal resolution and higher accuracy due to use of local data. Examples include OpenET (OpenET, 2021) and LANID (Xie et al., 2021) in the US, and TERN CMRSET in Australia available at 30 m spatial resolution (McVicar et al., 2022).

The spatial resolutions of global products range from 70 m to >1 km. PML\_V2 and MOD16A2 visual spectrum products were the only two available actual ET (ETa) products available globally at 500 m resolution, until the ECOSTRESS PT-JPL product was launched in 2018 at 70 m resolution (Guerschman et al., 2022)(Table 3). However, the short temporal coverage of ECOSTRESS is unsuitable for many applications. Finer spatial resolution products are necessary to understand crop variations and food security (Shi et al., 2014; Thenkabail et al., 2010). Global ET products do not exactly represent crop water requirements, and this needs to be considered when modelling irrigation for the WEFN.

Many ET data products merge RS with ground observations, land surface models that include data assimilation, and/or reanalysis (Liu et al., 2010; Guerschman et al., 2022; Peña-Arcibia and Ahmad, 2020; Zhang et al., 2019; Li et al., 2009; Courault et al., 2005). Thermal infrared (TIR) data are particularly useful in the majority of these methods, whilst visual based RS is also widely used, e.g. SSEBop (Senay et al., 2020) and MOD16A2 (Mu et al., 2011). Reference should be made to Li et al. (2009) and Zhang et al. (2016a), for more information on the methods, advantages and limitations of different ET calculation methods.

### 3.1.3. Streamflow

The WEFN is a recommended approach for developing trans-boundary river agreements (Keskinen et al., 2016; De Strasser et al., 2016; UNECE, 2015), and thus streamflow data are a necessity. RS, LSMs, or reanalyses alone do not provide reliable data for streamflow, although some global modelling efforts have produced streamflow data. The only openly available dataset providing streamflow measurements, requiring no hydrological modelling or analysis, is the Global Runoff Data Centre (GRDC) dataset, with data provided for over 100,000 stations (The Global Runoff Data Centre, 2020). However data coverage is not equally distributed across the world, and whilst some data are available from the 1800's to present, other stations are not up to date (The Global Runoff Data Centre, 2020). The Global Streamflow Indices and Metadata (GSIM) Archive also provides metadata on temporal and spatial availability and links for access to streamflow data (Do et al., 2018).

RS cannot reliably measure streamflow in ungauged basins, without hydrological modelling or *in situ* observations (Van Dijk et al., 2016). RS data can be used to supplement sparsely gauged river data in space and time (Pham et al., 2018) and for calibrating hydrologic models (Gleason and Durand, 2020). RS can also be used for prediction in ungauged basins through transfer functions relating streamflow data from geologically and climatologically similar gauged catchments (Jódar et al., 2018). Width/stage-discharge rating curves can be derived from fine spatial resolution RS, including Jason-2, MODIS, ENVISAT, and Landsat (Wang and Xie, 2018; Papa et al., 2012). The Surface Water and Ocean Topography Mission (SWOT) was launched in December 2022 and may contribute to improved understanding of streamflow. With three products, SWOT will monitor approximately 200,000 rivers with over 100 m width, with overpasses every 21 days (NASA, 2020). Although this is a relatively coarse temporal resolution, it should be useful for understanding seasonal streamflow dynamics at monthly scale for the WEFN.

An emerging area of research is the development of global streamflow reanalysis products and machine learning models for estimating global streamflow. These products are model derived, are generally at coarse spatial resolutions and can have substantial biases but may still be useful in terms of understanding seasonal dynamics or if *in situ* data are available for bias correction (Alfieri et al., 2020). GloFAS-ERA5 streamflow reanalysis covers the period 1979-present with a daily time step and 0.1 degree resolution (Harrigan et al., 2020). Lin et al. (2019) used RS, reanalysis, and a ground observation network to produce daily and monthly streamflow estimates at 2.94 million reaches from 1979 to 2014, in the Global Reach-level A priori Discharge Estimates for Surface Water and Ocean Topography (GRADES) product. The GRADES product was evaluated at approximately 14,000 gauges and although monthly correlations were generally high, there were substantial biases (>20%) at the majority of locations. Gridded monthly runoff data at 0.5 degree spatial resolution has also been estimated using machine learning covering the period from 1902 to 2014 (Ghiggi et al., 2021).

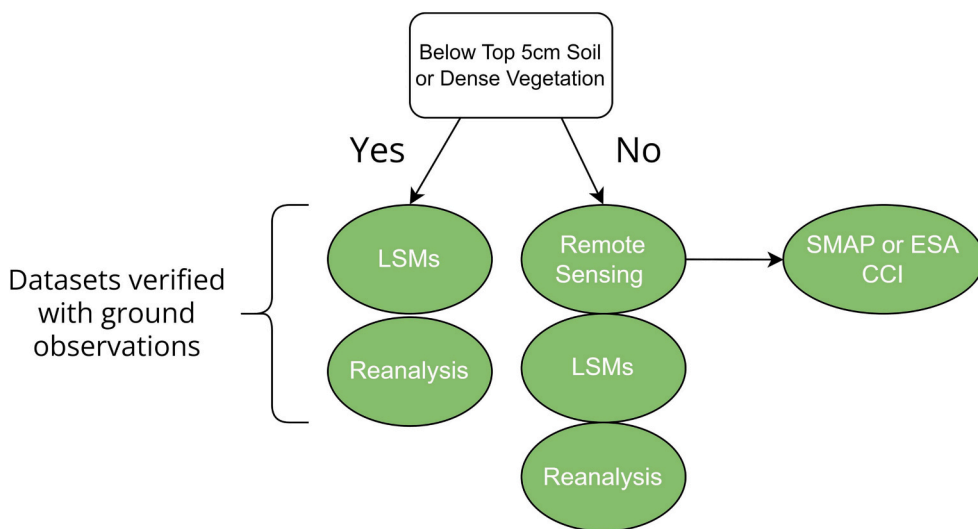


**Fig. 3.** Soil Moisture data hierarchy, based on depth of soil moisture of interest and vegetation.

**Table 4**  
Openly available soil moisture products available at the global level.

Data Product	Product Type	Spatial Resolution	Temporal Resolution	Spatial Coverage	Temporal Coverage	Reference
AMSR-E	RS	25 km	Daily	Global	2002–2011	N/A
AMSR-2	RS	10 km	Daily	Global	2012– present	N/A
ASCAT	RS	25–50 km	1.5 Days	Global	2007–present	(Wagner et al., 2013)
SMAP	RS	9 km	Daily	Global	2015– present	N/A
SMOS	RS	40–50 km	3-Days	Global	2009– present	N/A
GLDAS	LSM with data assimilated	0.25°/(1°)	3 Hourly	Global	2000–present/ (1979– present)	(Rodell et al., 2004)
SMAP L4 (below 5 cm)	Merged LSM and RS	9 km	Daily	Global	2015–present	(Entekhabi et al., 2010)
ESA CCI	Merged RS	0.25°	Daily	Global	1978– present	(Gruber et al., 2019)
MERRA2	Reanalysis	0.5°x0.625°	Hourly	Global	1980–present	(Gelaro et al., 2017)
ERA5	Reanalysis	0.28°	Hourly	Global	1950–present	(Muñoz-Sabater et al., 2021)
JRA55	Reanalysis	0.56°x0.5°	6 Hourly	Global	1958–present	(Kobayashi et al., 2015)

As precipitation data are more easily collected and hence, more widely available, basin scale hydrological models are most commonly used for estimating runoff in rivers, using the available precipitation data described above (Wang and Xie, 2018). RS can be used to determine inputs for hydrologic models, including for land-use, soil, vegetation, drainage, area, elevation and slope data (Coskun et al., 2010). Numerical modelling is not the focus of this paper, but an overview of different types of hydrological modelling available, and benefits and drawbacks of these models can be found in Fatichi et al. (2016), Sitterson et al. (2018), or Jaiswal et al. (2020). Despite attempts to calibrate hydrologic models without in situ data (Sun et al., 2015; Emery et al., 2018), such models generally still require calibration against ground observed records. Thus, some streamflow records are still required.

### 3.1.4. Soil moisture

Soil moisture information is important in irrigation scheduling for agriculture and in estimating runoff. There are generally three methods for estimating soil moisture content, including in situ measurements, LSMs, and RS. There are some in-situ networks of soil moisture data, including the Cosmic-ray Soil Moisture Observing System (COSMOS) (Zreda et al., 2012) and the International Soil Moisture Network (ISMN) (Dorigo et al., 2021). Njoku et al. (2003) concluded that ground networks are largely unsuitable for representing the high spatial and temporal variability of soil moisture and there has been limited improvements in terms of spatial or temporal coverage in the following 20 years. RS and LSMs with data assimilation can represent the spatial

and temporal variability well but introduce their own uncertainties.

Globally available soil moisture data includes RS, LSMs with data assimilation, and reanalysis products (Fig. 3). In most cases only the top 5 cm depth of soil moisture is measured by RS, and though this is used widely in RS soil moisture studies, the depth of the root zone in agriculture means that estimates of the top 5 cm soil moisture is likely insufficient for WEFN studies. Thus, LSMs with data assimilation (hereafter LSMs) are useful to understand soil moisture at greater depths, particularly where vegetation is dense (Nicolai-Shaw et al., 2015). GLDAS (an LSM) is used widely to estimate soil moisture over 5 cm depth and performs well (Spennemann et al., 2015).

Where RS is recommended (Fig. 3), SMAP should be considered first as it has outperformed other RS datasets in most cases globally and has higher spatial resolution than other products (Table 4) (Chen et al., 2018a; Fan et al., 2022; Kumar et al., 2018; Montzka et al., 2017). Additionally, SMAP Level 4 (L4) can estimate soil moisture deeper than 5 cm. If temporal coverage is required from before 2000, ESA CCI is recommended (Qiu et al., 2016; Li et al., 2022) (Table 4). In dense vegetation, the ability of microwave RS products are generally reduced (Duygu and Akyürek, 2019), although there have been cases where RS products perform well in dense vegetation (Kim et al., 2020), LSM products have been shown to perform more consistently over a range of dense vegetation (Fang et al., 2016).

### 3.1.5. Groundwater

Groundwater (GW) is water stored in soil and porous rock

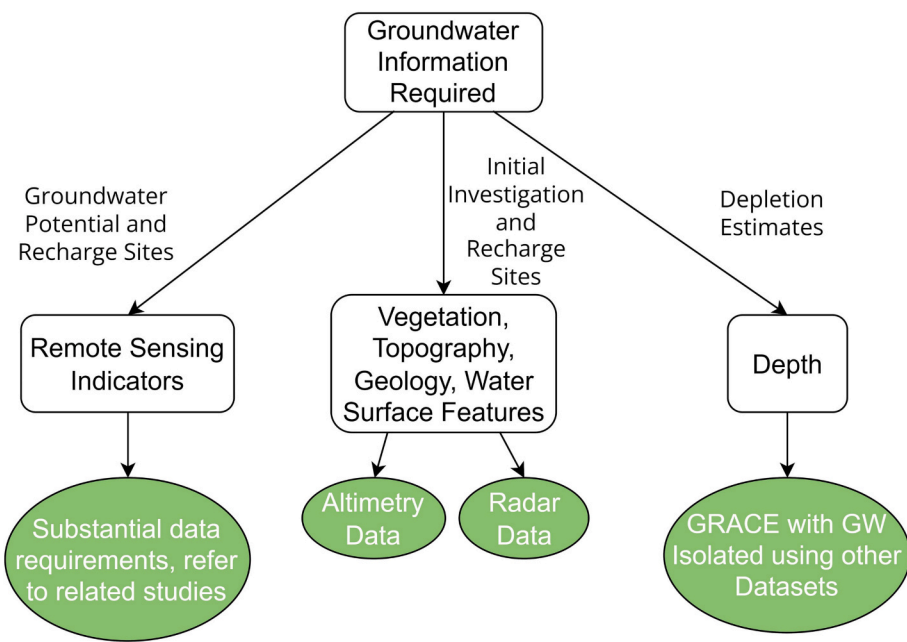


**Fig. 4.** Groundwater Data Proxies. Note none of the above products provide exact estimates of GW.

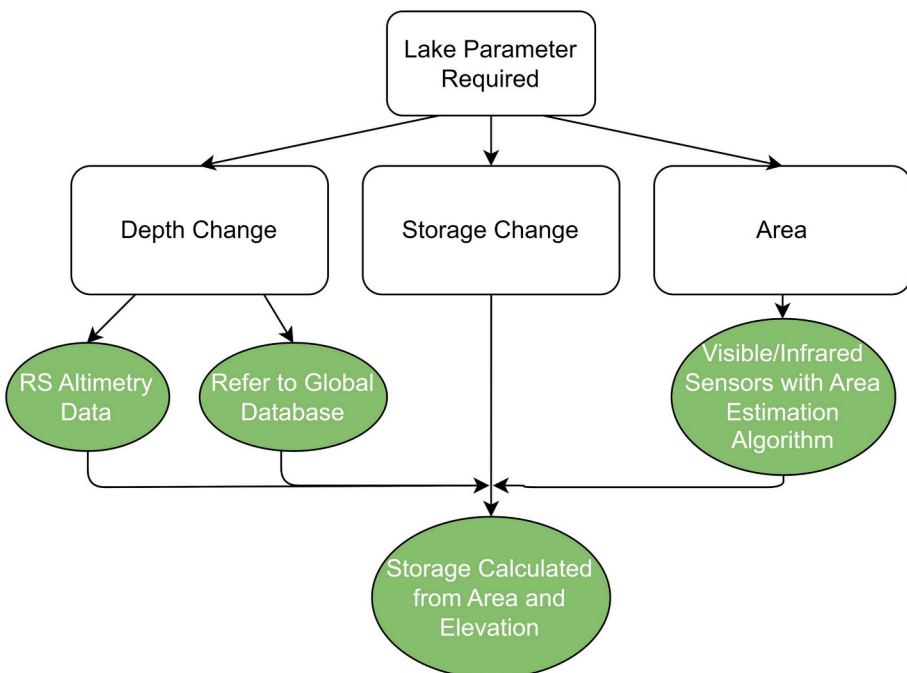


**Fig. 5.** Lake data hierarchy. RS is recommended for global estimations of lake area, level, and storage changes. With regards to depth changes, global databases which contain altimetry data should be referred to first. Area can be estimated from several sensors using algorithms discussed below. Using both altimetry and area data, storage changes can then be calculated.

underneath the Earth's surface, representing up to 33% of the world's water withdrawals (Siebert et al., 2010; Famiglietti, 2014). It is important as a primary drinking water source for much of the world's population and for irrigation water, but in many regions in the world it is poorly monitored (Famiglietti, 2014). Important considerations for groundwater from a WEFN perspective include surface water – GW interactions, the availability of GW, and understanding natural and artificial recharge (Jha et al., 2007). In situ observations are rarely available due to cost of installation and monitoring (Li et al., 2019). The only globally available global data source for GW measurements is the Global

Groundwater Information System (GGIS) which provides locations of transboundary aquifers, a global monitoring network, and sites of managed aquifer recharge (<https://ggis.un-igrac.org/>).

No global data currently exist to quantify GW availability, but RS can be used as a proxy (Fig. 4). More information on the use of RS for GW monitoring data generally, can be found in Becker (2006) and Jha et al. (2007). There have been no comprehensive reviews on global data for all GW information since 2007, with more recent reviews only considering one aspect of GW. Features important to GW availability such as topography, vegetation, springs and seeps can be detected and defined

**Table 5**

Openly available altimetry products. Note, although globally available, only a small percentage of lakes are currently captured by this data.

Satellite Mission	Temporal Resolution	Dates Active
ERS-1	35 days	1991–2000
ERS-2	35 days	1995–2011
Envisat	35 days	2002–2012
Jason-1	10 days	2001–2012
Jason-2	10 days	2008–2019
Jason-3	10 days	2016–present
Sentinel-3A&B	27 days	2016–present
ICESat	91 days	2003–2009
ICESat-2	91 days	2018–present

by RS imagery or radar data (Elbeih, 2015; Lillesand et al., 2015). RS can also be used to indicate possible recharge sites and potential, by assessing geomorphology, land use, lithology, lineament, soil, drainage density, river gradient and slope (e.g. Díaz-Alcaide and Martínez-Santos, 2019; Elewa and Qaddah, 2011; Oikonomidis et al., 2015; Srivastava and Bhattacharya, 2006; Jackson, 2002). These data have direct relevance to the WEFN from a water availability perspective.

GRACE and GRACE-FO have received substantial attention for measuring seasonal mass changes associated with overall water storage, including GW, soil moisture, surface water, snow, ice, intercepted water, and biomass (Li et al., 2019). GRACE data can be used to estimate interannual variability of GW worldwide in large catchments (Yeh et al., 2006; Frappart and Ramillien, 2018; Rodell et al., 2009), noting the need to isolate GW from other terrestrial water sources, thus relying on other hydrological information (Rodell et al., 2009). This makes GRACE post processing requirements substantial and limits its use in WEFN studies.

### 3.1.6. Lake/reservoir storage

Lakes and reservoirs (hereafter, lakes, encompassing both, without neglecting the importance of reservoir storage in the WEFN) with surface area > 50 km<sup>2</sup> cover more than 1.4% of global land surface (excluding Antarctica and glaciated Greenland) (Lehner and Döll, 2004).

**Table 6**

Openly available data for water surface area, available at the global level.

Satellite Sensor	Spatial Resolution	Temporal Resolution	Temporal Coverage
AVHRR	1.1 km	0.5 days	1978– present
Landsat (1–8)	15–120 m	16 days	1972– present
MODIS	250 m, 500 m, 1 km	Daily	1999– present
Sentinel 2	10 m, 20 m, 60 m	2–10 days	2015– present

**Table 7**

Openly available energy data, available at the global level. Also included are current energy installed and future targets of energy installation to achieve net-zero by 2030.

Energy Type	2019 Energy Generation (IEA, 2021)	Net-Zero Required Generation by 2030 (IEA, 2021)	Data Required	Data Available
Hydropower	4418 TWh	5870 TWh	Flow Elevation	See Section 3.1.3
Solar	821 TWh	6970 TWh	GHI DNI	Remote Sensing Reanalysis Global/National Atlas
Wind	Onshore 1592 TWh	8008 TWh	Wind Speed	Reanalysis Global/National Atlas
	Offshore		Wind Speed	Reanalysis Remote sensing
Geothermal	94 TWh	330 TWh	Thermally Stressed Vegetation	Remote Sensing
Bioenergy	718 TWh	1407 TWh	Individual Surface Features Agriculture Residue Energy	Remote Sensing National Statistics and literature
			Energy Crop Potential	Remote Sensing
			Forest Residue Energy	

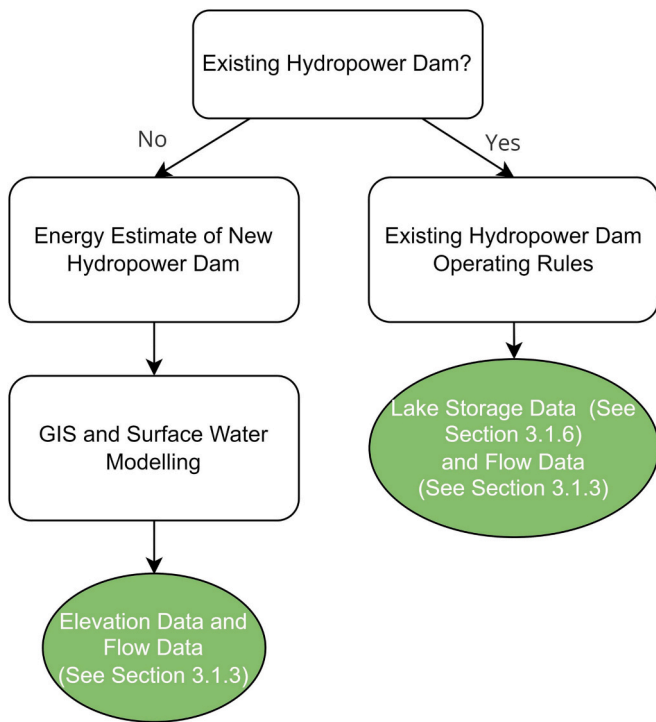


**Fig. 6.** Hydropower data hierarchy, based on globally available data. No readily available data currently exist, and reference should be made to appropriate sections.

Several RS products are available for mapping water surface area. SAR provides useful data in cases of darkness, cloud cover, and forest cover, however emergent vegetation and wind increase uncertainties (Smith, 1997). Passive microwave can also detect water under cloudy

conditions and dense vegetation, but spatial resolution is coarse (Gao, 2015; Ji et al., 2009). Passive visible/IR have been easily accessible, available at higher spatial and temporal resolutions, and provide good delineation if clouds, dense vegetation, and smoke do not obscure the water surface since at least the 1990's (Smith, 1997; Alsdorf et al., 2007; Ji et al., 2009). This is still the case and visible sensors are still widely used in water surface mapping, especially at large spatial scales, and coarse temporal resolutions. Such sensors include Landsat, MODIS, ASTER, and AVHRR (Table 6). Water features can be delineated from these sensors using several methods. Both NDWI and MNDWI have been successfully used (El-Shirbeny and Abutaleb, 2018; Duan and Bastiaanssen, 2013; Rokni et al., 2014; Sarp and Ozcelik, 2017). NDWI overestimates water area in built-up areas, thus where there is substantial anthropogenic development, MNDWI might be better (Xu, 2006).

### 3.2. Energy

Substantial increases in renewable energy generation are required globally to achieve net zero scenarios (IEA, 2021), to meet the SDGs (United Nations, 2021) and the Nationally Determined Contributions to the Paris Agreement to reduce greenhouse gas emissions (UNFCCC, 2022) (Table 7). Thus, this section will focus on onshore renewable energy (hydropower, solar, wind, geothermal, and biomass). Offshore wind resources are also considered due to their similarities with onshore wind, fast development and current prominence in national policies worldwide (IEA, 2019). The key data of interest for energy development are the theoretical availabilities of the resources which produce the energy, for example for wind power, wind speed is assessed. There are several data sources available for most sectors (Table 7). Practical constraints, such as proximity to grid or topography are important, but these considerations and therefore the data for these aspects are outside the scope of this paper.

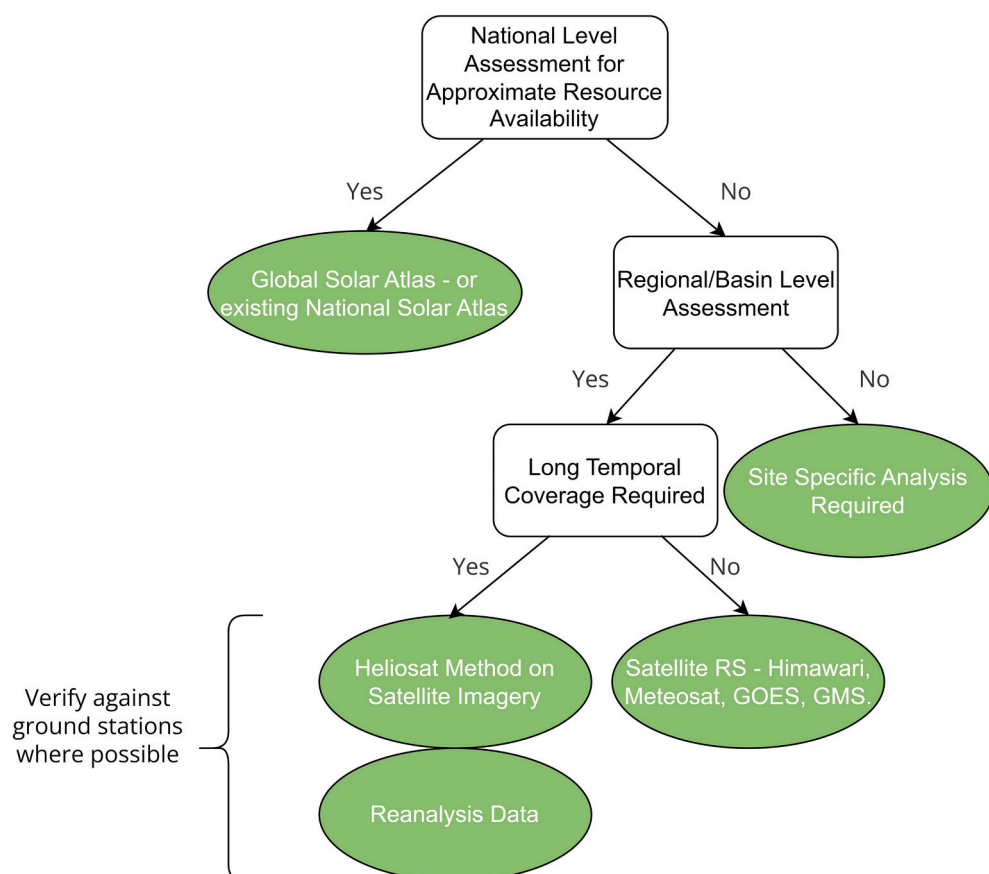


**Fig. 7.** Solar Power data hierarchy, based on openly available data sources. "Long temporal coverage" represents temporal coverage prior to 2010.

**Table 8**

Openly available solar irradiance products. HELIOSAT databases, satellites, reanalysis, and near-global to global databases are detailed below. Only GOES has a method advised, as this method is commonly used for the satellite coverage.

Dataset Type	Dataset	Spatial Resolution	Temporal Resolution	Spatial Coverage	Temporal Coverage	Source
Database	HELIOLIM (HELIOSAT)	~3-10 km	Sub-hourly	+/- 66° Long/Lat	2004-present	(Blanc et al., 2011)
Database	SARAH (HELIOSAT)	0.05°	Daily- Monthly	+/- 65° Long/Lat	1983-2017	(Müller et al., 2015, Pfeifroth et al., 2019)
Satellite	Himawari (Any Method)	1-2 km	Sub-hourly	E/SE Asia and Oceania	1977-Present	N/A
Satellite	METEOSAT (Any Method)	1-3 km	Sub-hourly	+/- 60° Long/Lat	1977- Present	N/A
Satellite	NOAA GOES (PSM V3)	2-4 km	Sub-hourly	Americas	1998- Present	N/A
Reanalysis	MERRA-2	0.5°	Hourly	Global	1979-Present	(Gelaro et al., 2017)
Reanalysis	ERA5	0.28°	Hourly	Global	1950-Present	(Hersbach et al., 2020)
Reanalysis	JRA-55	0.56°	3-Hourly	Global	1959- Present	(Kobayashi et al., 2015)
Reanalysis	GSA	250 m-1 km	Annual	60°N-45°S	Varies	(Global Solar Atlas, 2019a)
Reanalysis	NSRDB	4 km	Typical Year	60°N-60°S	Varies	(Sengupta et al., 2018)
Reanalysis	NSRDB	2-10 km	Sub-hourly – hourly	60°N-60°S	Varies	(Sengupta et al., 2018)

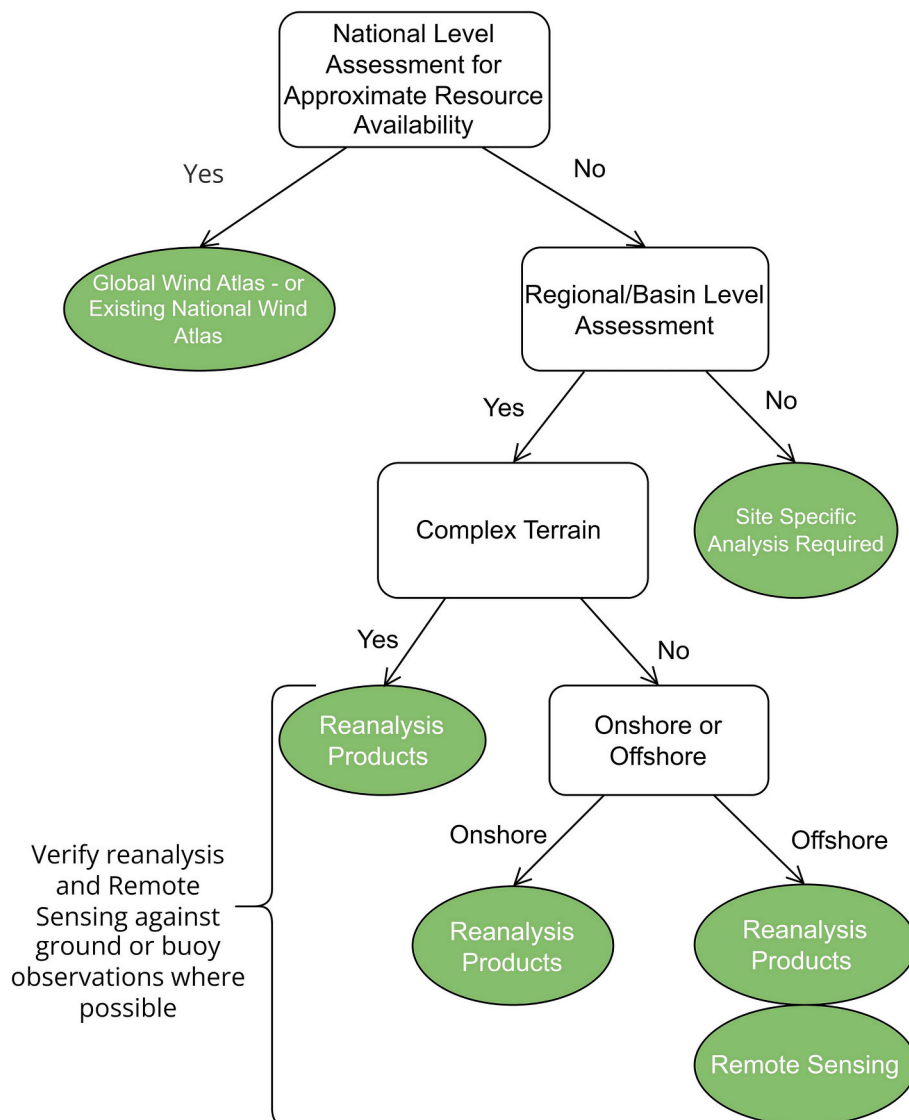


**Fig. 8.** Wind data hierarchy, based on globally openly available data. GWA is only recommended to assess feasibility of wind for country scale. Reanalysis is generally recommended for analysis after this. Although remote sensing has some capability in offshore wind speed, it is not useful for onshore assessments. Complex terrain is characterised by uneven topography, for example including mountainous regions.

**Table 9**

Openly available global scale wind energy data products.

Resource	Dataset/ Satellite Mission	Spatial Resolution	Temporal Resolution	Spatial Coverage	Temporal Coverage	Source
Onshore/ Offshore	ERA5	0.28°	Hourly	Global	1950-Present	(Hersbach et al., 2020)
Onshore/ Offshore	JRA-55	0.56°	3-Hourly	Global	1959- Present	(Kobayashi et al., 2015)
Onshore/ Offshore	MERRA-2 *	0.5°	Hourly	Global	1979-Present	(Gelaro et al., 2017)
Offshore	ASCAT	25-50 km	1.5 Days	Global	2007-present	N/A
Offshore	QuikSCAT	25 km	daily	Global	1999-2009	N/A

### 3.2.1. Hydropower

Hydropower has been the centre of many WEFN studies (Basheer et al., 2021; Yang et al., 2018; Jalilov et al., 2015). As well as energy generation, hydropower dams have multiple benefits and impacts on water and food sectors. There are two main data needs, including the theoretical potential energy available from new hydropower and the operating rules of existing hydropower dams (Fig. 6). However, because of its strong commercial relevance, data are rarely shared on hydropower operations.

The theoretical potential of hydropower is primarily dependent on flow and elevation head (Coskun et al., 2010; Larentis et al., 2010; Kusre et al., 2010). Flow data have been discussed in Section 3.1.3, which concluded that there are currently limited globally available data sources for flow, these limited data sources are unlikely to be available for the exact point of interest. Because streamflow data are usually unavailable from global sources at points of interest, hydrological modelling has been necessary (Coskun et al., 2010; Kusre et al., 2010; Pandey et al., 2015). Elevation head could be considered using a Digital Elevation Model (DEM), showing topography, which thus could be used to measure the elevation differences between mountains and valleys where hydropower is being considered. There are a wide range of DEMs available, including for example, the Shuttle Radar Topography Mission (SRTM) from NASA at 30 or 90 m resolution, between 60°N and 50°S (USGS, 2018). For national scale assessments, it may be sufficient to assess whether hydropower is a feasible option for energy generation using only precipitation, evapotranspiration, and elevation data, however these hydropower energy estimates will not be precise. Operating rules govern how water is released from reservoirs. In the absence of publicly available operating rules, flow, lake drawdown, and lake area are required (Fig. 6) (Section 3.1.3 and 3.1.6). The limitation of flow data also limits the ability to understand hydropower operating rules of hydropower at points of interest.

### 3.2.2. Solar energy

Solar energy capacity in 2030 has to be more than eight times the capacity in 2019 (Table 7) to achieve net-zero (IEA, 2021). Solar energy encompasses solar thermal heating and solar photovoltaic energy (Solar PV). In both cases, Solar Surface Irradiance (SSI) is the primary driver of the potential energy resource. SSI is made up of three variables, Direct Normal Irradiance (DNI), Diffuse Horizontal Irradiance (DHI) and Global Horizontal Irradiance (GHI) (Qin et al., 2021). DNI and GHI are the two most important components for estimating potential solar energy resources (Lopes et al., 2018). DNI and GHI can be determined in three ways, including via numerical modelling, ground observations, or satellite RS (Jia et al., 2021). The uncertainty of all products usually increases under cloudy conditions (Damiani et al., 2018; Zhao et al., 2013; Huang et al., 2019).

For estimating availability of solar energy at national scale, the Global Solar Atlas (GSA), or an existing national solar atlas is recommended first (Fig. 7). Although the spatiotemporal resolution of GSA is not high, it is easy to use and suitable to determine whether solar resources are viable in an area of interest, although it should not be used for detailed investigation. In GSA, uncertainties are higher for DNI, higher latitudes, regions with high aerosols, coastal zones, humid climates, regions with low data quality or no data availability, and snow- or ice-covered mountainous regions in particular (Global Solar Atlas,

2019b).

At sub-national level, satellite RS is recommended (Fig. 7). The National Solar Radiation Database (NSRDB) is a good near-global database, which has estimates of typical year solar irradiance and provides some data at finer temporal resolutions from recent geostationary satellites, namely METEOSAT, HIMAWARI, and GOES (<https://nsrdb.nrel.gov/>). Geostationary satellites are generally recommended for current solar irradiance data because of their fine spatiotemporal resolutions (Hirooka et al., 2018; Bessho et al., 2016) and collectively, they cover most of the globe. The temporal coverage of many recent solar irradiance products using these satellites is however limited, typically not beginning before 2000. There are many methods available for use with RS information, including physical process based methods and statistical methods (Huang et al., 2019).

The HELIOSAT method has been widely used in solar energy estimation (Table 8). HELIOSAT derived databases and reanalysis are recommended if data before 2010 are required. However, reanalysis is often not as accurate as RS products (Vindel et al., 2016; Huang et al., 2020; Zhang et al., 2016b; Yu et al., 2019). Several different HELIOSAT methods have been applied to imagery from METEOSAT (Hammer et al., 2003; Hammer et al., 1999), Fengyun-4A (Jia et al., 2021), and Himawari (Han and Vohnicky, 2022). Generally, HELIOSAT has higher uncertainties in cloudy conditions, near coasts and tropical areas due to cloud formations, and at higher latitudes (Eissa et al., 2015; Blanc et al., 2011). GHI is usually better represented than DNI in HELIOSAT (Eissa et al., 2015; Jia et al., 2021).

### 3.2.3. Wind energy

Wind energy can be harvested through wind turbines located on land (onshore) or over water (offshore). Wind energy is more difficult to estimate over large areas compared to solar energy due to its substantial spatial heterogeneity from land use, altitude, and topography (Murthy and Rahi, 2017, Zhou et al., 2011, Eurek et al., 2017, Keyhani et al., 2010). The most accurate way of collecting wind resource data is via in situ anemometer measurements, placed on masts at turbine height. However, wind turbines are being constructed taller, thus, placing anemometers at turbine height is becoming more difficult. Existing measurements are spatially sporadic (Monaldo et al., 2001). Because wind energy is proportional to the cube of the wind speed, errors in wind speed measurements result in large errors in wind energy output (Arun Kumar et al., 2020).

To assess feasibility of resources at national scales, the global wind atlas (GWA) (<https://globalwindatlas.info/>) is useful, despite its low spatiotemporal resolution. Any analysis considering more detail would require higher precision in energy output estimates, and GWA would be inappropriate for this (Fig. 8).

Reanalysis is widely used for energy estimates of both offshore and onshore resources (Staffell and Pfenninger, 2016; Gruber et al., 2022; Rabbani and Zeeshan, 2020), and thus is recommended when finer than national scale availability is required. However, reanalysis products have large uncertainties, and generally need to be corrected with ground observations. Thus, reanalysis should be approached with caution in study locations with sparse data (Rabbani and Zeeshan, 2020; Fan et al., 2021). Complex topography, including mountainous regions, coastal areas and lower wind speeds are not as well represented by reanalysis (Jourdier, 2020; Rabbani and Zeeshan, 2020; Gualtieri, 2022), temporal

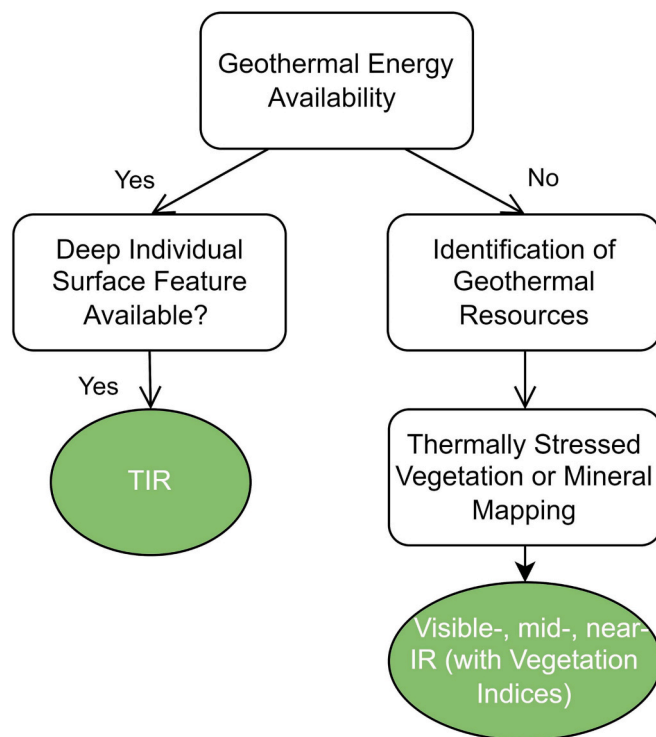


**Fig. 9.** Geothermal data hierarchy based on globally, openly available data. Only where deep individual surface features can be detected and analysed, can resource availability be estimated. Otherwise, RS can only be used for identifying areas for further investigation.

aggregation to the monthly values appropriate for WEFN analyses substantially improves data reliability (Gruber et al., 2022). However, the spatial resolution of reanalysis is still relatively coarse (Table 9). Reference should be made to Fan et al. (2021) and Miao et al. (2020) when considering which reanalysis product performs best for any particular region. If detailed or precise wind resource assessments are needed, reanalysis data can be coupled with a computational fluid dynamics model to understand complex flows induced by surrounding topography (Kim et al., 2018; Waewsak et al., 2019).

RS is only useful to estimate offshore wind resources (Young et al., 2020; Hasager et al., 2008; Monaldo et al., 2001). There are several satellite products available for estimating wind speed, including SAR products, scatterometers, altimeters, and passive microwave radiometers (Young et al., 2020; Hasager et al., 2008). It is generally recommended to use multiple satellites in wind resource assessments, to reduce uncertainty and improve the temporal resolution (Wei et al., 2019). However, in situ observations are still required to validate the offshore RS wind products prior to use in wind energy estimation (Hasager et al., 2008).

### 3.2.4. Geothermal energy

The temperature gradient in the Earth's crust is usually 25–30 °C/km depth, however in volcanic zones, this can increase to up to 150 °C/km depth (Van der Meer et al., 2014). Within a depth of 10 km from the Earth's surface, geothermal resources can produce the equivalent energy of  $3 \times 10^{17}$  billion barrels of oil, theoretically meeting global energy requirements for the next six million years (Lund et al., 2008).

Satellite RS can be used in the initial stages of investigations but in situ surveys are required to precisely measure geothermal energy potential (Qin et al., 2011). There are two ways to assess geothermal resources availability using RS (Fig. 9). VIs are recommended for mapping thermally stressed vegetation and different growth rates, which can indicate CO<sub>2</sub> vents from geothermal systems (Bateson et al., 2008).

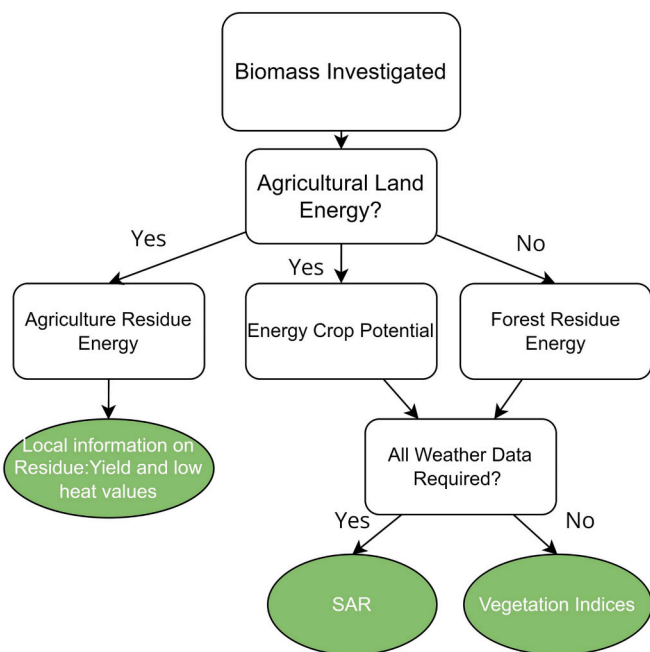


**Fig. 10.** Biomass data hierarchy, based on globally openly available data. National statistics are necessary for residue estimation.

**Table 10**

Biomass Satellite Missions, including optical and radar. Note: many radar products are only available by request, if downloading fine spatial resolution data.

Dataset/ Satellite Mission	Spatial Resolution	Temporal Resolution/revisit time	Temporal Coverage
ALOS PALSAR	10-100 m	N/A	2005-present
AVHRR	1.1 km	0.5 days	1978-present
ENVISAT ASAR	1 km	35 days	2002–2012
Landsat	15-120 m	16 days	1972- present
MODIS	250 m, 500 m, 1 km	Daily	1999-present
RADARSAT	5-500 m	N/A	1995-present
Sentinel-1	1.7 m × 4.3 m – 15 m × 43 m	6–12 days	2014-present
SPOT	1.5-20 m	1–3 days	1986- present

Minerals can also suggest the presence of geothermal resources (Kratt et al., 2010). RS for both vegetation and minerals rely on visible-, mid-IR, and near-IR channels to identify areas of potential resources although both methods have led to false positives in the past (Kratt et al., 2010; Bateson et al., 2008). Other direct and indirect indicators of geothermal resources include temperature, gas emissions, surface deformation, hot springs, fumaroles, and calderas (Haselwimmer and Prakash, 2013).

Surface features can be used to estimate temperature and the energy potential of underground resources, although these have large uncertainties (Vaughan et al., 2012; Heasler and Jaworowski, 2018). TIR can estimate surface temperature and geothermal heat flux, but surface features are usually tens of meters in dimension (Mongillo et al., 1995), and thus most current satellites do not have high enough spatial resolution (Heasler and Jaworowski, 2018).

### 3.2.5. Biomass

Biomass accounts for 35% and 3% primary energy needs in developing and developed countries, respectively (Avtar et al., 2019). Biomass can come from agricultural by-products, forests, and dedicated energy crops (Fig. 10). Energy from agricultural by-product, or residual energy, cannot be accurately determined directly by any globally

**Table 11**

Crop Information Datasets grouped according to application. Useful in WEFN modelling for irrigation estimates, crop area, crop productivity, and food output estimation.

Dataset/ Satellite Mission	Applications	Spatial Resolution	Temporal Resolution	Temporal Coverage	Reference
AVHRR (optical)	Crop Area	1.1 km	0.5 days	1978-present	N/A
MODIS (optical)	Crop Growth	250 m, 500 m, 1 km	Daily	1999-present	N/A
Landsat (optical)	Irrigation mapping	15-120 m	16 days	1972- present	N/A
Envisat (MERIS)	Crop Growth	~300 m	35 days	2002-2012	N/A
SMAP	Irrigation mapping	9 km	Daily	2015- present	N/A
Sentinel-1 (C-band SAR)	Crop area	2.3 m × 14.1 m	12 days	2014-present	N/A
AMSR-E (Passive MW)	Crop Growth	0.25°	Daily	2002-2011	N/A
AMSR-2 (Passive MW)		10 km	Daily	2012- present	N/A
GOSAT FTS (SIF)		10.5 km	3 days	2009- present	N/A
MetOp (GOME-2) (SIF)		0.5°	monthly	2007-present	N/A
FLEX (SIF)		300x300m	27 days	Not Launched	N/A
MOD13A3	NDVI	1 km	Monthly	2000-present	(Didan, 2015)
MOD13C1	EVI	0.05°	16-days	2000-present	(Didan, 2015)
AVH15C1	Global LAI Product	0.05°	Daily	1981-present	(Claverie et al., 2016)
GLASS		1 km	8-day	2000-present	(Ma and Liang, 2022)
GIAM (RS Based)	Irrigation product	1 km	N/A	2000	(Thenkabail et al., 2009)
GMIA (census)		5 arc min	N/A	2000-2008	(Siebert et al., 2013)
GRIPPC (Census and RS)		500 m	N/A	2005	(Salmon et al., 2015)
LGRIP		30 m	N/A	2015	(Teluguntla et al., 2023)
MIRCA2000 (Census and RS)		5 arc min	N/A	2000	(Portmann et al., 2010)
GLCC	Global Land Cover Map	1 km	N/A	1992-1993	(EROS, 2018)
WorldCover		10 m	N/A	2020-2021	(Zanaga et al., 2022)
GlobeLand30		30 m	N/A	2000, 2010, 2020	(Jun et al., 2014)

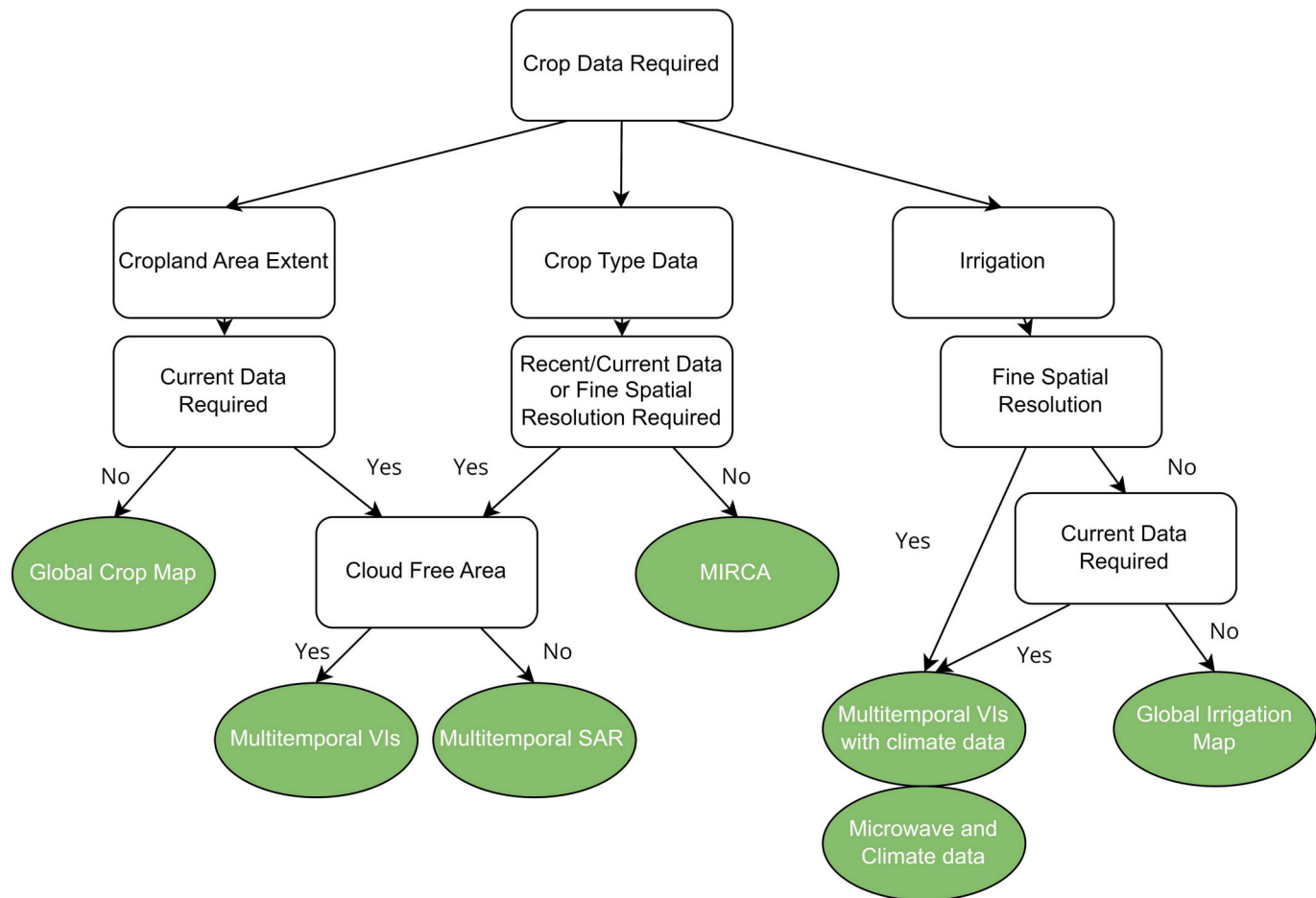


**Fig. 11.** Crop Area data hierarchy based on globally openly available data. Note that finer spatial resolution represents sub-kilometre spatial resolution.

available products. Therefore, to estimate the residual energy potential, local or regional data on biomass residue are required, along with yield and heat energy values to estimate energy potential (Gao et al., 2016; Jiang et al., 2019; Hiloidhari et al., 2014; Angelis-Dimakis et al., 2011). To calculate above ground biomass, radar and optical sensors can be used with VIs and statistical models (Kumar et al., 2015; Lu, 2006; Ahamed et al., 2011; Gonçalves et al., 2021).

VIs can be derived from optical RS based on the changes of reflectance, emanating from changes to biomass production (Ahamed et al., 2011). VIs are however specific to species, conditions, and vegetation type (Viña et al., 2011), meaning VIs employed at large scale might not represent biomass well without processing. VIs are also sensitive to cloud cover, with relatively high uncertainty, whereas SAR data are suitable for almost all-weather conditions, making it especially good for crops which grow in wet seasons, e.g. rice (Chao et al., 2019). Optical data uncertainties result from the inability to assess biomass structural uncertainty, heterogeneity, and seasonality (Kumar and Mutanga, 2017). Optical sensing is good for assessing horizontal canopy cover and vegetation types. However there are limitations in estimating canopy height (Kumar et al., 2015), which is especially important in forests. A list of satellite products for biomass is provided (Table 10).

### 3.3. Food

Food demand is increasing rapidly, with global crop demand expected to grow by up to 110% between 2005 and 2050 (Tilman et al., 2011). As a result, large areas of land will potentially have to be cleared with associated increases in irrigated areas required (Tilman et al., 2011). Food as a sector is a strong driver of both water and energy use, with 70% of global water used for irrigation, and 30% of global energy used for food production and supply (FAO, 2014). Food data are often available through national statistics offices, though the data usually do not cover all crop types and there is limited information on the spatial or temporal distribution of resources. Satellite RS presents a good alternative to address these limitations.

The focus of this section is on crop area and yield which can be estimated using a variety of methods (Table 11). Crop area and yield are the variables directly representing resource availability at the regional and catchment scale considered here. At the local scale, crop yield is affected by pests, disease, soil nutrient availability, and meteorological conditions (Karthikeyan et al., 2020). For more information on how RS can be used for monitoring crop pests and diseases, refer to the review by Mutanga et al. (2017). For more information on how RS data can be used as a proxy for food security, including access to available food, refer to Brown (2016).

#### 3.3.1. Crop area

Satellite imagery has been widely used to map cropland, although crop area is sometimes difficult to estimate due to its high spatiotemporal variability and ground data necessary to distinguish different crop types (Shi et al., 2014; Brown, 2016). To estimate crop area, three types of data are of interest: overall crop extent, crop type, and irrigated area (Fig. 11).

To estimate cropland extent, the 10 m spatial resolution WorldCover product, available for 2020–2021 (Zanaga et al., 2022), is the finest spatial resolution product available (Table 11), followed by the Global Cropland-Extent Product at 30-m Resolution (GCEP30), using Landsat data and VIs (Thenkabail et al., 2021). Notably, several products for cropland extent, irrigation area, and crop classification have severely limited temporal coverage, with many only available for nominal years (Table 11).

If crop classifications are required, the MIRCA2000 dataset, with 26 crop classes available, is useful, although the spatial resolution is 5 arc min, and it is only available for around the year 2000 (Portmann et al., 2010). If more recent and/or higher spatial resolution is required on crop types then global maps are inadequate. In this case, multitemporal

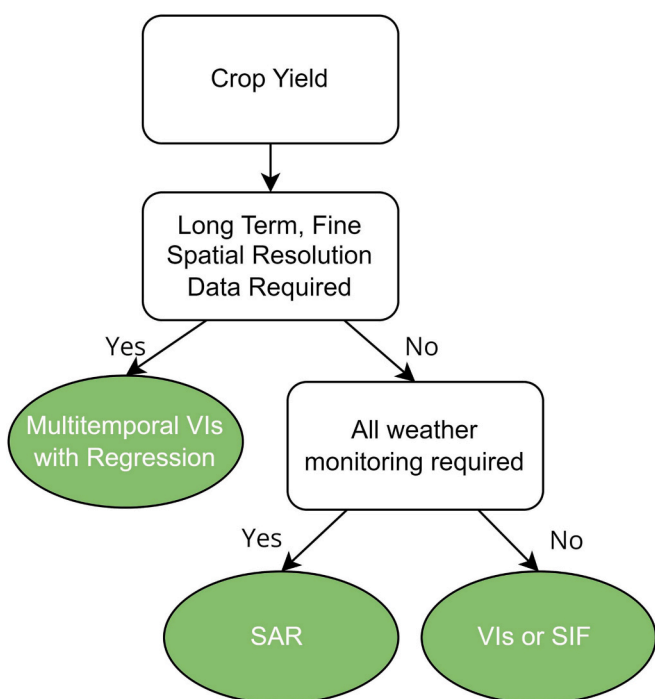


Fig. 12. – Crop Yield data hierarchy based on globally openly available data.

SAR or VIs are recommended. Several images are required because it is difficult to distinguish between crop types based on single images (Shi et al., 2022). Both SAR and VIs have performed well in estimating overall crop extent and individual crop areas (McNairn et al., 2014; Steele-Dunne et al., 2017; Jia et al., 2012; Chen et al., 2020; Guiomar et al., 2021; Xiao et al., 2005). SAR have increasingly improved spatial resolution which has meant they are capable of capturing more heterogeneous farming (Chen et al., 2020). SAR data are available in all weather conditions and at night. It can thus assess temporal variations of cropland and is becoming increasingly popular for crop classification (Shi et al., 2022; Skriver et al., 2011; Kim et al., 2012; McNairn and Shang, 2016). Thus, SAR is better applied to crops in cloudy areas, or grown in the rainy season, whilst VIs are well suited to cloud free conditions, or where longer temporal gaps in data are acceptable.

For irrigation mapping, visible, NIR, LSMS, and microwave data can all be used (Massari et al., 2021). Visible and NIR can be used to understand irrigation extent, frequency, and timing, from local to global scale, at spatial scales up to 30 m using Landsat and MODIS using VIs and/or ancillary data (Ozdogan et al., 2006; Beltran and Belmonte, 2001; Biggs et al., 2006; Chen et al., 2018b). For assessing irrigated areas, multiple images over time are also usually required (Ozdogan et al., 2006; Beltran and Belmonte, 2001). NDVI has been used to map irrigated areas with high accuracy (Ozdogan et al., 2006; Beltran and Belmonte, 2001; Biggs et al., 2006). Microwave detected soil moisture has also provided promising results in identifying irrigated areas (Qiu et al., 2016; Lawston et al., 2017). There are also several global irrigation products which were produced for years between 2000 and 2015 (Table 11).

#### 3.3.2. Crop yield

There are three useful methods for approximating crop yield, including linear regression models with VIs, Solar Induced Fluorescence (SIF), and active microwave (Fig. 12)(Mulla, 2013; Guan et al., 2017; Kenduiywo et al., 2018; Kim et al., 2012; Mohammed et al., 2019; Guan et al., 2016). The performances of the methods are affected by a range of variables, including crop type, length of training data, atmospheric variables, and soil type (Peng et al., 2020; Karthikeyan et al., 2020).

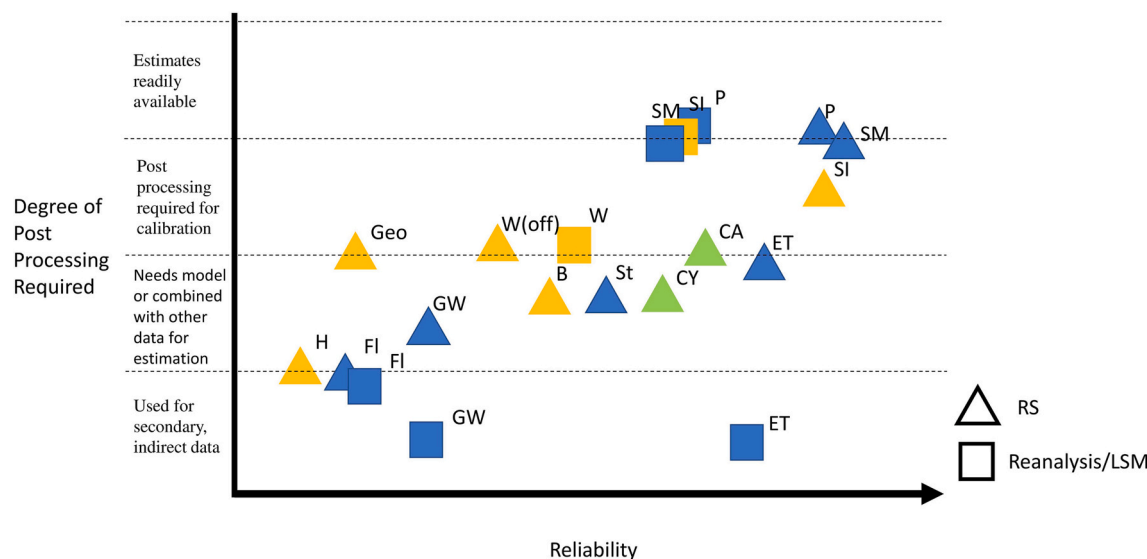


**Fig. 13.** WEFN Global Data Source Capability for Water (blue), Energy (yellow), and Food (green). Point shapes represent data source types – triangle for satellite remote sensing (RS) and square for reanalysis or land surface models (LSM) datasets. Streamflow data which are currently not globally available is represented by a circle. Reliability (x-axis) is a qualitative measure of how much uncertainty is inherent in the datasets based on literature reviewed. The y-axis represents the amount of post-processing required to use the datasets for WEFN modelling. P-Precipitation, ET-Evapotranspiration, SM-Soil Moisture, St-Lake Storage, FI-Streamflow, CA – Crop Area, CY – Crop Yield, SI-Solar irradiance, W-Wind, W(off)-Offshore wind, B-Biomass, H-Hydropower, Geo-Geothermal Energy. (For interpretation of the references to colour in this figure legend, the reader is referred to the web version of this article.)

Food crop yield – i.e., the yield of the crop which is used as food – cannot be precisely estimated without some form of numerical modelling or ground-based data for first establishing an empirical relationship. Thus, although, RS can be used alone to broadly compare difference in yields in a given area, it will not give precise values for food crop yield alone.

Regression based methods with VIs are commonly used for crop yield estimates, particularly where long term data with high spatial resolution are required (Guan et al., 2017). There is a strong relationship between crop yield and VIs, especially in the later part of the growing season, although local ground data are required to first establish these empirical relationships (Labus et al., 2002; Quaraby et al., 1993; Lai et al., 2018; Mirasi et al., 2021). The combination of NIR and red bands and of NIR and green bands perform especially well in crop yield studies (Mulla, 2013; Labus et al., 2002). Using several VI observations over time generally improves results (Labus et al., 2002; Lai et al., 2018). Hyper- and multi-spectral images can also be used to estimate crop yield and have showed promising results (Kira et al., 2016; Wu et al., 2010; Mulla, 2013). Using multiple sensors and various spectral ranges can also improve yield estimates (Guan et al., 2017).

Leaf Area Index (LAI) is also closely related with yield and is a common input into crop models (Doraiswamy et al., 2005; Mokhtari et al., 2018; Doraiswamy et al., 2004). There are several ways to calculate LAI using satellite RS, mainly via optical and microwave sensors with empirical relationships or algorithms. Fang et al. (2019) provides a good overview of these and more uses of LAI generally. LAI can also be estimated via microwave and LiDAR, with LiDAR available from ICESat used with radiative transfer models, and radar backscatter used with empirical relationships (Fang et al., 2019). Global LAI products have higher uncertainties in tropical and boreal regions as well as in summer seasons (Fang et al., 2019).

Solar Induced Chlorophyll Fluorescence (SIF) emissions are a more direct indicator of photosynthesis compared with VIs and other indicators (Mohammed et al., 2019, Guan et al., 2016). However, SIF measurements are not currently practical for WEFN assessments due to their coarse resolution (Mohammed et al., 2019; Peng et al., 2020) and the need for supplementary numerical modelling to process the data

(Yang et al., 2019). The Fluorescence Explorer (FLEX) mission will provide higher resolution estimates of SIF when launched in 2025 (Drusch et al., 2017). With the FLEX mission and more research, this could be a viable option in the future.

Another project which may improve food data reliability is the Global Food Security-Support Analysis Data 30 m resolution (GFSAD30) project which aims to monitor crop dynamics from 2000 to 2025, producing maps with cropland types and spatial and temporal intensities (Olivant et al., 2022; Western Geographic Science Center, 2018).

Active microwave is also influenced by crop variables, and can be used to estimate crop structure, crop growth, LAI, water content, and biomass (Kenduiywo et al., 2018; Kim et al., 2012). SAR is the most widely used radar due to its relatively fine spatial resolutions, although it is still too coarse for representing highly spatially variable crop planting practices (Steele-Dunne et al., 2017). A benefit of radar is the ability to provide information on the entire canopy, not constrained to the top layer of leaves (Kim et al., 2012). As for crop area, SAR can provide crop yield monitoring under all weather conditions (Mcnairn and Shang, 2016).

## 4. Discussion

### 4.1. Overall synthesis of WEFN data availability and suitability

RS, reanalysis, and LSMs all provide data useful for WEFN modelling but with varying reliability and post-processing requirements (Fig. 13). Overall, no sector is better represented than any other by global data sources. RS can represent more variables (thirteen) and with better reliability than either LSMs or reanalysis (seven). The best represented variables are soil moisture, precipitation, and solar irradiance. The largest gaps in global datasets (Fig. 13) are streamflow, groundwater, hydropower, and geothermal resources. This ranking is based on the literature available, how much and the complexity of post-processing required overall, and the relative precision of products without calibration. The relative reliability is based on the literature stating to what extent variables can be estimated. I.e., the variables ranked lower are

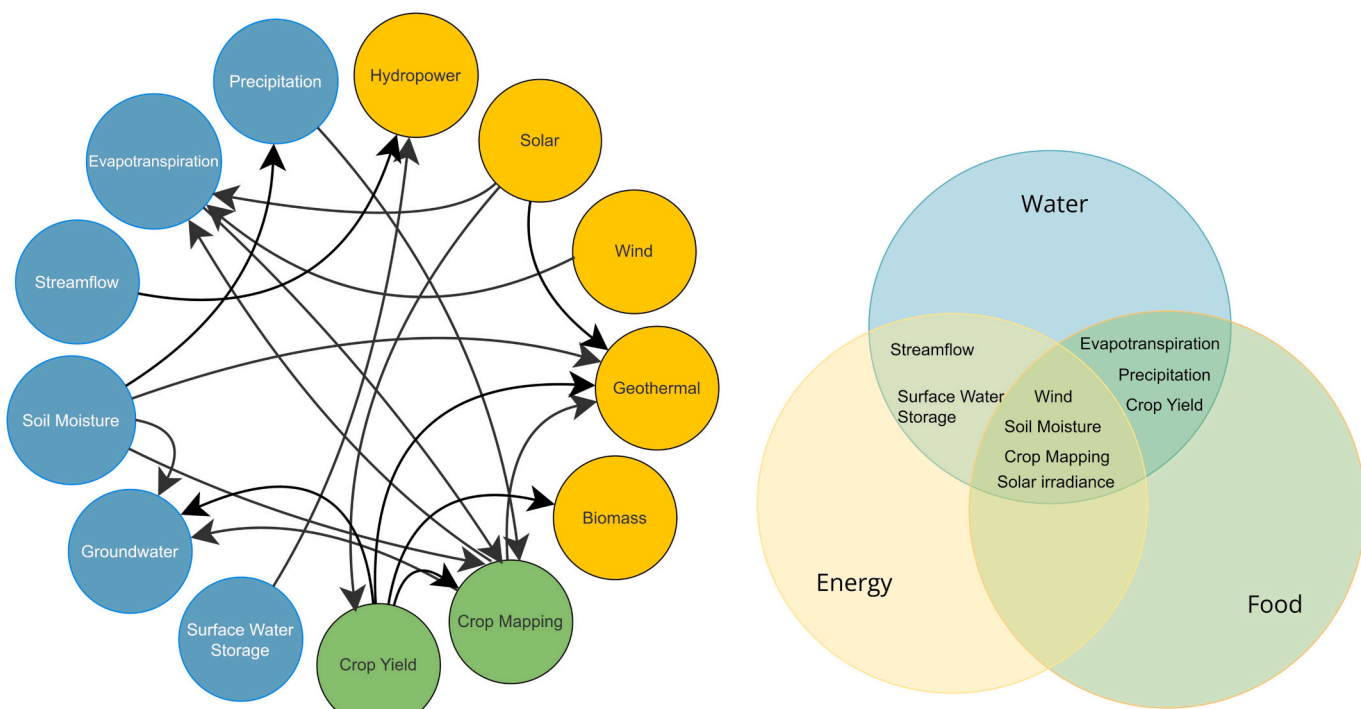


**Fig. 14.** a Direct data synergies between the natural and human system variables involved in the WEFN (left) where each circle represents a variable and they are coloured according to their primary sectoral classification (blue – water, yellow – energy and green – food), and Fig. 14b - Data Nexus overlaps (right). (For interpretation of the references to colour in this figure legend, the reader is referred to the web version of this article.)

only useful for initial scoping investigations because of the high or undefined uncertainty associated with the data, whilst the variables ranked higher provide estimates with quantified uncertainties.

It is important to remember that all the global data sources discussed here are modelled to varying degrees, from relatively simple algorithms or linear regression to complex numerical models. Thus, all data products have included some ground data for calibration and validation at some point during their development. The ranking here is thus focused on how much additional post-processing or local ground data are required by WEFN modellers to provide useful estimates of variables influencing the nexus.

Precipitation and soil moisture are best represented by global datasets. Whilst solar irradiance is also represented well it was ranked lower than precipitation and soil moisture (Fig. 13), due to the widespread use of geostationary satellites which are not global. ET, crop area, and crop yield data are also reliably estimated by global products, however, the data provided usually need to be combined with other data products (e.g., LSMs or reanalysis) or land observations and are therefore ranked as requiring more post-processing for WEFN modelling. Crop area was ranked higher than crop yield because total combined crop area maps can be produced without in situ data, whereas crop yield for food relies on local ground data for correction. Wind, lake storage, and biomass are ranked around the middle of the 13 variables (Fig. 13). Storage is not truly globally available, with a very low percentage of lakes measured by altimeters and in global databases, and hence ranked lower in both reliability and post-processing. Wind data have high uncertainties, and biomass requires other data to calculate the required energy estimates. Streamflow RS and reanalysis data were ranked low, as both can only be used with complex numerical models to provide estimates, and most data outputs have large uncertainties unless corrected with in situ data, which are rarely available.

Hydropower is often central in WEFN studies (Basheer et al., 2021; Yang et al., 2018; Jalilov et al., 2015; Vinca et al., 2021a). The limited availability of streamflow data leads to a lack of data on hydropower

potential and operating rules. Although SWOT (Section 3.1.3) will improve this, data will likely still not be available at potential new hydropower dam sites or directly downstream of existing hydropower dam sites. Even national streamflow datasets may not be sufficient. Therefore, it is likely that some form of hydrological modelling will continue to be required in WEFN studies.

#### 4.2. WEFN variable interactions

In this sub-section the focus is specifically on WEFN data interactions in the context of the review and not on the larger system interactions that are a key feature of the WEFN. In particular, global data for one variable sometimes contributes to global data sources for another variable. The synergies in Fig. 14 have been identified based on the literature review undertaken here, where one variable was directly necessary and/or beneficial in the global data calculation of a second variable. These data interactions can be uni-directional or bi-directional (Fig. 14). For example, soil moisture and precipitation are widely used for RS irrigation mapping (Massari et al., 2021; Qiu et al., 2016; Brown, 2016), depicted as a uni-directional interaction. Bi-directional interactions occur between ET and crop mapping because crop mapping products are used in some ET products, but likewise, ET along with other meteorological products are sometimes used in irrigation mapping products. However, although hydropower data are relevant information for agriculture at a local scale, global agricultural data, i.e., NDVI, do not use hydropower data as a direct input. Thus, hydropower is not considered a direct data interaction for agriculture. There are obviously many more interactions between variables, for example since wind affects ET, it will also then impact streamflow in a hydrologic model, as a second-order model interaction. Here only primary global data interactions are considered, which is the first time that such interactions have been explicitly mapped for the WEFN.

Improving global data for one WEFN variable can benefit other variables' global data. For example, in investigating geothermal

resources, it is important to remove solar radiation, soil moisture, and vegetation fluxes to minimize false positives (Qin et al., 2011; Coolbaugh et al., 2007). Wind data are important for ET numerical models and global ET estimations (Courault et al., 2005; Gomis-Cebolla et al., 2019). But reanalysis wind speed is unreliable and presents challenges in ET calculations when using reanalysis products (Nouri and Homaei, 2022), thus improvement of wind data can benefit ET. Solar irradiance is important in solar energy estimation, but also contributes to ET estimates (Huang et al., 2019). Variable interactions are also important to understand uncertainties in estimates of the WEFN sectors individually and collectively. The interactions mean that data uncertainties can cascade through the WEFN if global data for one variable are used in another variable's global data calculation. For example, uncertainties in precipitation datasets could affect crop mapping which in turn impact geothermal energy estimates.

There is an urgent need for a WEFN-focused database that can manage data interactions at local and global scales as well as the multi-disciplinary nature of WEFN studies. The database should include all the globally available variables reviewed here. A monthly temporal resolution would balance the need to represent seasonal and interannual variability but also maximise data availabilities, as some variables are not monitored at finer temporal resolution. Such a database would be beneficial for basin- to national-scale rapid assessment of nexus interactions in near-future decision making and planning. For example, if food availability is low in a region, there is no benefit in assessing energy crop biomass. Further analysis and modelling would still be required for full WEFN implementation, but global maps could assist in this rapid nexus assessment.

The multi-disciplinary nature of WEFN studies makes a user-friendly database interface necessary, for example by combining the global data through map layers. With WEFN associated international agencies as custodians and suitable investment, this could be in the form of a data repository, however, this requires substantial effort. Thus, failing this, a referral service to the appropriate water, energy, or food data output data online is also recommended. As highlighted in Fig. 13, global data often require expertise in post-processing. With the number of disciplines involved in the WEFN, data collection and presentation are complex, and both decision makers and researchers will be required to work outside of their main area expertise. A map-based interface could assist under these conditions.

#### 4.3. Priorities for data improvements for WEFN modelling

Considering the direct data interactions within the WEFN summarised in this review (Fig. 14), there are clear priority areas for data collection. Soil moisture, crop mapping and solar irradiance are central in the WEFN (Fig. 14b), but existing global data sources can capture the variables relatively well, compared with other variables. Wind speed has also been allocated a central role in the nexus due to its importance in ET calculations for irrigation. Wind speed data have high uncertainties which have large consequences for the WEFN, considering that 70% of water is used for food production globally (FAO, 2014). Wind speed is thus considered a priority area in the WEFN global data improvement. Considering only global data interactions, streamflow data are only relevant in global water and energy data; however, it is considered a priority area for the WEFN, due to its impact on hydropower calculations which are central to many WEFN studies. Wind estimation and streamflow both currently require substantial post processing and/or numerical modelling from global data sources considered here to create location specific, precise estimates.

Thus, currently ground, national and multilateral agency level, and other data sources are required for WEFN implementation. Variables where global data are currently insufficient include streamflow, groundwater, crop yield, biomass, geothermal energy, and hydropower energy. This requirement cascades into other global data calculation (Fig. 14), therefore ground networks and other data sources must

continue to be maintained and improved. Notably, Geographic Information Systems (GIS) are useful tools for managing data for the WEFN. Although the focus of the review here was mainly on temporally varying variables, static variables often best managed in GIS can also complement the data discussed here. For example, river streamflow and reservoirs/lakes GIS datasets, showing locations and vectors for dams and rivers, including, MERIT- Hydro (Yamazaki et al., 2019), SWORD (Altenau et al., 2021), and GeodAR (Wang et al., 2022). National and multilateral level data collection are also imperative from a WEFN perspective to supplement the gaps in global data products. National Statistics Offices often report on past crop yield and area data, as well as meteorological data with varying variables and resolutions. National meteorological offices collect and often share some hydrological data, although the data publicly available online varies. Multilateral agencies, such as the World Meteorological Organization (WMO), IRENA, and FAO, collect and publish data on water, energy, and food, respectively.

#### 5. Conclusion

This review of global data sources has synthesized and recommended data sources for modelling the WEFN, whilst highlighting priority areas for WEFN global data sources. The data hierarchies presented will assist data prioritisation and collection efforts for WEFN researchers, practitioners, and policy makers with specific relevance for enhancing progress towards national SDG and net zero targets across each of the water, energy, and food sectors. Implementation of WEFN modelling using openly available global datasets allows national and transboundary consideration of SDGs 2, 6, and 7, even for locations where ground observation data are unavailable or inadequate for assessment.

The recommendations for priority areas are based on current gaps in data availability as well as the synergies that exist in global data. Streamflow, wind speed, and hydropower are priority areas in the WEFN that are not currently suitably monitored by global data sources. Crop yield, biomass, geothermal energy, and groundwater, also require additional data or post processing before use. Furthermore, although global data sources can monitor many WEFN variables, spatial and temporal scale discrepancies between variables and sectors still exist, particularly with respect to the coarse spatial resolution of data. Due to the synergies between global data sources here, a combined database for WEFN assessments would be beneficial to better integrate decision making and homogenise the different data sources. Interactions between variables and their uncertainties were highlighted as they are vital to represent correctly in WEFN modelling.

Considering the number of variables which still require additional data for estimation, national and multilateral institution data are still needed for WEFN modelling. National and multilateral institution data can complement the data collected from the global data sources discussed here for calibration and validation. Thus, ground networks and the associated databases must continue to be maintained and improved in the future in parallel with global data improvements. The data hierarchies and recommendations presented here provide an insight into the data available for WEFN implementation in locations where data scarcity is still prevalent.

#### Declaration of Competing Interest

The authors declare that they have no known competing financial interests or personal relationships that could have appeared to influence the work reported in this paper.

#### Data availability

Table 12 provides a list of URLs for data sources mentioned above. In the "Data Information" column are links to home pages for datasets, or pages which provide a brief description of data. In the "Data URL" column, there are URLs to data download pages. There are some databases

Table 12 Data websites and downloading platforms.

Product	Data Information	Data URL
ALOS PALSAR	<a href="https://www.eorc.jaxa.jp/ALOS/">https://www.eorc.jaxa.jp/ALOS/</a>	<a href="https://gportal.jaxa.jp/">https://gportal.jaxa.jp/</a>
AMSR-2	<a href="https://www.eorc.jaxa.jp/AMSR/satellite/">https://www.eorc.jaxa.jp/AMSR/satellite/</a> <a href="https://www.earthdata.nasa.gov/eosdis/sips/amsr-sips">https://www.earthdata.nasa.gov/eosdis/sips/amsr-sips</a>	<a href="https://gportal.jaxa.jp/">https://gportal.jaxa.jp/</a>
AMSR-E	<a href="https://www.eorc.jaxa.jp/AMSR/satellite/">https://www.eorc.jaxa.jp/AMSR/satellite/</a> <a href="https://www.earthdata.nasa.gov/eosdis/sips/amsr-sips">https://www.earthdata.nasa.gov/eosdis/sips/amsr-sips</a>	<a href="https://gportal.jaxa.jp/">https://gportal.jaxa.jp/</a>
ASCAT	<a href="https://www.eumetsat.int/ascat">https://www.eumetsat.int/ascat</a>	<a href="https://navigator.eumetsat.int/search">https://navigator.eumetsat.int/search</a> <a href="https://search.earthdata.nasa.gov/">https://search.earthdata.nasa.gov/</a>
AVHRR	<a href="https://www.earthdata.nasa.gov/sensors/avhrr">https://www.earthdata.nasa.gov/sensors/avhrr</a>	<a href="https://search.earthdata.nasa.gov/">https://search.earthdata.nasa.gov/</a> <a href="https://earthexplorer.usgs.gov/">https://earthexplorer.usgs.gov/</a>
Climate Prediction Center (CPC)	<a href="https://www.cpc.ncep.noaa.gov/">https://www.cpc.ncep.noaa.gov/</a>	<a href="https://search.earthdata.nasa.gov/">https://search.earthdata.nasa.gov/</a> <a href="https://earthexplorer.usgs.gov/">https://earthexplorer.usgs.gov/</a>
CMORPH	<a href="https://www.ncei.noaa.gov/products/climate-data-records/precipitation-cmorphon-cmorph">https://www.ncei.noaa.gov/products/climate-data-records/precipitation-cmorphon-cmorph</a>	<a href="https://www.ncei.noaa.gov/data/cmorph-high-resolution-global-precipitation-estimates/access/">https://www.ncei.noaa.gov/data/cmorph-high-resolution-global-precipitation-estimates/access/</a>
ECOSTRESS PT-JPL	<a href="https://ecostress.jpl.nasa.gov/">https://ecostress.jpl.nasa.gov/</a>	<a href="https://search.earthdata.nasa.gov/">https://search.earthdata.nasa.gov/</a> <a href="https://earthexplorer.usgs.gov/">https://earthexplorer.usgs.gov/</a>
Envisat	<a href="https://earth.esa.int/eogateway/missions/envisat">https://earth.esa.int/eogateway/missions/envisat</a>	<a href="https://earth.esa.int/eogateway/search">https://earth.esa.int/eogateway/search</a>
ERA5	<a href="https://www.ecmwf.int/en/forecasts/dataset/ecmwf-reanalysis-v5">https://www.ecmwf.int/en/forecasts/dataset/ecmwf-reanalysis-v5</a>	<a href="https://cds.climate.copernicus.eu/">https://cds.climate.copernicus.eu/</a>
ERS-1	<a href="https://earth.esa.int/eogateway/missions/ers">https://earth.esa.int/eogateway/missions/ers</a>	<a href="https://earth.esa.int/eogateway/search">https://earth.esa.int/eogateway/search</a>
ERS-2	<a href="https://earth.esa.int/eogateway/missions/ers">https://earth.esa.int/eogateway/missions/ers</a>	<a href="https://earth.esa.int/eogateway/search">https://earth.esa.int/eogateway/search</a>
ESA CCI	<a href="https://esa-soilmoisture-cci.org/">https://esa-soilmoisture-cci.org/</a>	<a href="https://climate.esa.int/en/odp/#/project/soil-moisture">https://climate.esa.int/en/odp/#/project/soil-moisture</a>
FLEX (SIF)	<a href="https://earth.esa.int/eogateway/missions/flex">https://earth.esa.int/eogateway/missions/flex</a>	<a href="https://earth.esa.int/eogateway/tools/esov-software-tools-esov-ng">https://earth.esa.int/eogateway/tools/esov-software-tools-esov-ng</a>
GIAM	<a href="https://waterdata.iwmi.org/applications/giam2000/">https://waterdata.iwmi.org/applications/giam2000/</a>	<a href="https://waterdata.iwmi.org/applications/giam2000/">https://waterdata.iwmi.org/applications/giam2000/</a>
GLASS	<a href="http://www.glass.umd.edu/introduction.html">http://www.glass.umd.edu/introduction.html</a>	<a href="http://www.glass.umd.edu/Download.html">http://www.glass.umd.edu/Download.html</a>
GLCC	<a href="https://www.usgs.gov/centers/eros/science/usgs-eros-archive-land-cover-products-global-land-cover-characterization-glcc">https://www.usgs.gov/centers/eros/science/usgs-eros-archive-land-cover-products-global-land-cover-characterization-glcc</a>	<a href="https://earthexplorer.usgs.gov/">https://earthexplorer.usgs.gov/</a>
GLDAS	<a href="https://ldas.gsfc.nasa.gov/gldas">https://ldas.gsfc.nasa.gov/gldas</a>	<a href="https://search.earthdata.nasa.gov/search">https://search.earthdata.nasa.gov/search</a> <a href="https://disc.gsfc.nasa.gov/datasets?keywords=GLDAS">https://disc.gsfc.nasa.gov/datasets?keywords=GLDAS</a>
GLEAM V3.6a	<a href="https://www.gleam.eu/">https://www.gleam.eu/</a>	<a href="https://www.gleam.eu/">https://www.gleam.eu/</a>
GLEAM V3.6b	<a href="https://www.gleam.eu/">https://www.gleam.eu/</a>	<a href="https://www.gleam.eu/">https://www.gleam.eu/</a>
Global Precipitation Climatology Centre (GPCC)	<a href="https://www.dwd.de/EN/ourservices/gpcc/gpcc.html">https://www.dwd.de/EN/ourservices/gpcc/gpcc.html</a>	<a href="https://opendata.dwd.de/climate_environment/GPCC/html/download_gate.html">https://opendata.dwd.de/climate_environment/GPCC/html/download_gate.html</a>
Global Precipitation Climatology Project (GPCP)	<a href="https://disc.gsfc.nasa.gov/datasets/GPCPDAY_3.1/summary">https://disc.gsfc.nasa.gov/datasets/GPCPDAY_3.1/summary</a>	<a href="https://search.earthdata.nasa.gov/">https://search.earthdata.nasa.gov/</a>
GlobeLand30	<a href="http://www.globallandcover.com/">http://www.globallandcover.com/</a>	<a href="http://www.globallandcover.com/">http://www.globallandcover.com/</a>
GMIA	<a href="https://www.fao.org/aquastat/en/geospatial-information/global-maps-irrigated-areas/latest-version">https://www.fao.org/aquastat/en/geospatial-information/global-maps-irrigated-areas/latest-version</a>	<a href="https://www.fao.org/aquastat/en/geospatial-information/global-maps-irrigated-areas/latest-version">https://www.fao.org/aquastat/en/geospatial-information/global-maps-irrigated-areas/latest-version</a>
GOSAT	<a href="https://www.gosat.nies.go.jp/en/index.html">https://www.gosat.nies.go.jp/en/index.html</a>	<a href="https://data2.gosat.nies.go.jp/">https://data2.gosat.nies.go.jp/</a>
GSA	<a href="https://globalsolaratlas.info/map">https://globalsolaratlas.info/map</a>	<a href="https://globalsolaratlas.info/map">https://globalsolaratlas.info/map</a>
GSMaP	<a href="https://sharaku.eorc.jaxa.jp/GSMaP/guide.html">https://sharaku.eorc.jaxa.jp/GSMaP/guide.html</a>	<a href="https://gportal.jaxa.jp/gpr/">https://gportal.jaxa.jp/gpr/</a> <a href="https://sharaku.eorc.jaxa.jp/GSMaP/index.htm">https://sharaku.eorc.jaxa.jp/GSMaP/index.htm</a>
HELIOCCLIM	<a href="https://www.soda-pro.com/help/helioclim/helioclim-3-overview">https://www.soda-pro.com/help/helioclim/helioclim-3-overview</a>	<a href="https://www.soda-pro.com/help/helioclim/helioclim-3-overview">https://www.soda-pro.com/help/helioclim/helioclim-3-overview</a>
Himawari	<a href="https://www.data.jma.go.jp/mscweb/data/himawari/">https://www.data.jma.go.jp/mscweb/data/himawari/</a>	<a href="https://www.data.jma.go.jp/mscweb/en/himawari89/cloud_service/cloud_service.html">https://www.data.jma.go.jp/mscweb/en/himawari89/cloud_service/cloud_service.html</a>
ICESat	<a href="https://icesat.gsfc.nasa.gov/icesat/">https://icesat.gsfc.nasa.gov/icesat/</a>	<a href="https://search.earthdata.nasa.gov/">https://search.earthdata.nasa.gov/</a> <a href="https://nsidc.org/data/icesat/data">https://nsidc.org/data/icesat/data</a>
ICESat-2	<a href="https://icesat-2.gsfc.nasa.gov/">https://icesat-2.gsfc.nasa.gov/</a>	<a href="https://search.earthdata.nasa.gov/">https://search.earthdata.nasa.gov/</a> <a href="https://nsidc.org/data/icesat-2/data">https://nsidc.org/data/icesat-2/data</a>
IMERG	<a href="https://gpm.nasa.gov/data/imerg">https://gpm.nasa.gov/data/imerg</a>	<a href="https://search.earthdata.nasa.gov/">https://search.earthdata.nasa.gov/</a> <a href="https://gpm.nasa.gov/data/directory">https://gpm.nasa.gov/data/directory</a>
Jason-1	<a href="https://podaac.jpl.nasa.gov/JASON1">https://podaac.jpl.nasa.gov/JASON1</a>	<a href="https://podaac.jpl.nasa.gov/JASON1">https://podaac.jpl.nasa.gov/JASON1</a>
Jason-2	<a href="https://podaac.jpl.nasa.gov/OSTM-JASON2">https://podaac.jpl.nasa.gov/OSTM-JASON2</a>	<a href="https://www.ncei.noaa.gov/products/jason-satellite-products">https://www.ncei.noaa.gov/products/jason-satellite-products</a>
Jason-3	<a href="https://sealevel.jpl.nasa.gov/missions/jason-3/summary/">https://sealevel.jpl.nasa.gov/missions/jason-3/summary/</a>	<a href="https://www.ncei.noaa.gov/products/jason-satellite-products">https://www.ncei.noaa.gov/products/jason-satellite-products</a>
JRA55	<a href="https://jra.kishou.go.jp/JRA-55/">https://jra.kishou.go.jp/JRA-55/</a>	<a href="https://jra.kishou.go.jp/JRA-55/index_en.html">https://jra.kishou.go.jp/JRA-55/index_en.html</a>
Landsat	<a href="https://landsat.gsfc.nasa.gov/">https://landsat.gsfc.nasa.gov/</a>	<a href="https://earthexplorer.usgs.gov/">https://earthexplorer.usgs.gov/</a>
LGRIP	<a href="https://lpdaac.usgs.gov/products/lgrip30v001/">https://lpdaac.usgs.gov/products/lgrip30v001/</a>	<a href="https://lpdaac.usgs.gov/tools/earthdata-search/">https://lpdaac.usgs.gov/tools/earthdata-search/</a>
MERRA2	<a href="https://gmao.gsfc.nasa.gov/reanalysis/MERRA-2/">https://gmao.gsfc.nasa.gov/reanalysis/MERRA-2/</a>	<a href="https://search.earthdata.nasa.gov/">https://search.earthdata.nasa.gov/</a> <a href="https://disc.gsfc.nasa.gov/datasets?project=MERRA-2">https://disc.gsfc.nasa.gov/datasets?project=MERRA-2</a>
METEOSAT	<a href="https://www.eumetsat.int/our-satellites/meteosat-series">https://www.eumetsat.int/our-satellites/meteosat-series</a>	<a href="https://navigator.eumetsat.int/search">https://navigator.eumetsat.int/search</a>
MetOp	<a href="https://www.eumetsat.int/metop">https://www.eumetsat.int/metop</a>	<a href="https://navigator.eumetsat.int/search">https://navigator.eumetsat.int/search</a>
MIRCA2000	<a href="https://www.fao.org/land-water/land/land-governance/land-resources-planning-toolbox/category/details/en/c/1032166/">https://www.fao.org/land-water/land/land-governance/land-resources-planning-toolbox/category/details/en/c/1032166/</a>	<a href="https://www.uni-frankfurt.de/45218031/data_download">https://www.uni-frankfurt.de/45218031/data_download</a>
MOD13A3	<a href="https://lpdaac.usgs.gov/products/mod13a3v006/">https://lpdaac.usgs.gov/products/mod13a3v006/</a>	<a href="https://search.earthdata.nasa.gov/">https://search.earthdata.nasa.gov/</a>
MOD13C1	<a href="https://lpdaac.usgs.gov/products/mod13c1v006/">https://lpdaac.usgs.gov/products/mod13c1v006/</a>	<a href="https://search.earthdata.nasa.gov/">https://search.earthdata.nasa.gov/</a>
MOD16A2	<a href="https://lpdaac.usgs.gov/products/mod16a2v006/">https://lpdaac.usgs.gov/products/mod16a2v006/</a>	<a href="https://modis.gsfc.nasa.gov/data/">https://modis.gsfc.nasa.gov/data/</a> <a href="https://earthexplorer.usgs.gov/">https://earthexplorer.usgs.gov/</a>
MODIS	<a href="https://modis.gsfc.nasa.gov/">https://modis.gsfc.nasa.gov/</a>	<a href="https://www.gloh2o.org/mswep">https://www.gloh2o.org/mswep/</a>
Multi-Source Weighted-Ensemble Precipitation, Version 2 (MSWEP V2)	<a href="https://www.gloh2o.org/mswep/">https://www.gloh2o.org/mswep/</a>	
NOAA GOES (PSM V3)	<a href="https://nsrdb.nrel.gov/data-sets/us-data">https://nsrdb.nrel.gov/data-sets/us-data</a>	<a href="https://nsrdb.nrel.gov/data-viewer">https://nsrdb.nrel.gov/data-viewer</a>
NSRDB	<a href="https://nsrdb.nrel.gov/data-viewer">https://nsrdb.nrel.gov/data-viewer</a>	<a href="https://nsrdb.nrel.gov/data-viewer">https://nsrdb.nrel.gov/data-viewer</a>

(continued on next page)

(continued)

Product	Data Information	Data URL
NTSG	<a href="https://www.umt.edu/numerical-terrodynamic-simulation-group/project/global-et.php">https://www.umt.edu/numerical-terrodynamic-simulation-group/project/global-et.php</a>	<a href="https://www.umt.edu/numerical-terrodynamic-simulation-group/project/global-et.php">https://www.umt.edu/numerical-terrodynamic-simulation-group/project/global-et.php</a>
PERSIANN	<a href="https://chrsdata.eng.uci.edu/">https://chrsdata.eng.uci.edu/</a>	<a href="https://chrsdata.eng.uci.edu/">https://chrsdata.eng.uci.edu/</a>
PERSIANN CCS-CDR	<a href="https://chrsdata.eng.uci.edu/">https://chrsdata.eng.uci.edu/</a>	<a href="https://chrsdata.eng.uci.edu/">https://chrsdata.eng.uci.edu/</a>
PERSIANN-CDR	<a href="https://chrsdata.eng.uci.edu/">https://chrsdata.eng.uci.edu/</a>	<a href="https://chrsdata.eng.uci.edu/">https://chrsdata.eng.uci.edu/</a>
PML_V2	<a href="https://www.sciencedirect.com/science/article/pii/S003442571830590X#ac0005">https://www.sciencedirect.com/science/article/pii/S003442571830590X#ac0005</a>	<a href="https://code.earthengine.google.com/?asset=projects/pml_evapotranspiration/PML/OUTPUT/PML_V2_8day_v014">https://code.earthengine.google.com/?asset=projects/pml_evapotranspiration/PML/OUTPUT/PML_V2_8day_v014</a> <a href="https://github.com/kongdd/PML">https://github.com/kongdd/PML</a>
QuikSCAT	<a href="https://podaac.jpl.nasa.gov/QuikSCAT">https://podaac.jpl.nasa.gov/QuikSCAT</a>	<a href="https://podaac.jpl.nasa.gov/QuikSCAT">https://podaac.jpl.nasa.gov/QuikSCAT</a>
RADARSAT	<a href="https://www.asc-csa.gc.ca/eng/satellites/radarsat/">https://www.asc-csa.gc.ca/eng/satellites/radarsat/</a>	<a href="https://www.eodms-sgdot.nrcan-rncan.gc.ca/index-en.html">https://www.eodms-sgdot.nrcan-rncan.gc.ca/index-en.html</a> <a href="https://earth.esa.int/eogateway/missions/radarsat#data-section">https://earth.esa.int/eogateway/missions/radarsat#data-section</a>
SARAH (HELIOSAT)	<a href="https://data.europa.eu/data/datasets/eo-eum-cm-mult-sarah_v002?local_e=en">https://data.europa.eu/data/datasets/eo-eum-cm-mult-sarah_v002?local_e=en</a>	<a href="https://wui.cmsaf.eu/safira/action/viewDoiDetails?acronym=SARAH_V002">https://wui.cmsaf.eu/safira/action/viewDoiDetails?acronym=SARAH_V002</a>
SEBS	<a href="https://data.tpdc.ac.cn/en/data/df4005fb-9449-4760-8e8a-09727df9fe36/">https://data.tpdc.ac.cn/en/data/df4005fb-9449-4760-8e8a-09727df9fe36/</a>	<a href="https://data.tpdc.ac.cn/en/data/df4005fb-9449-4760-8e8a-09727df9fe36/">https://data.tpdc.ac.cn/en/data/df4005fb-9449-4760-8e8a-09727df9fe36/</a>
Sentinel-1	<a href="https://sentinel.esa.int/web/sentinel/missions/sentinel-1">https://sentinel.esa.int/web/sentinel/missions/sentinel-1</a>	<a href="https://scihub.copernicus.eu/">https://scihub.copernicus.eu/</a> <a href="https://navigator.eumetsat.int/search">https://navigator.eumetsat.int/search</a>
Sentinel-2	<a href="https://sentinel.esa.int/web/sentinel/missions/sentinel-2">https://sentinel.esa.int/web/sentinel/missions/sentinel-2</a>	<a href="https://scihub.copernicus.eu/">https://scihub.copernicus.eu/</a> <a href="https://navigator.eumetsat.int/search">https://navigator.eumetsat.int/search</a>
Sentinel-3A&B	<a href="https://sentinels.copernicus.eu/web/sentinel/missions/sentinel-3">https://sentinels.copernicus.eu/web/sentinel/missions/sentinel-3</a>	<a href="https://scihub.copernicus.eu/">https://scihub.copernicus.eu/</a> <a href="https://navigator.eumetsat.int/search">https://navigator.eumetsat.int/search</a>
SMAP	<a href="https://smap.jpl.nasa.gov/">https://smap.jpl.nasa.gov/</a>	<a href="https://nsidc.org/data/smap/data">https://nsidc.org/data/smap/data</a>
SMOS	<a href="https://earth.esa.int/eogateway/missions/smso">https://earth.esa.int/eogateway/missions/smso</a>	<a href="https://earth.esa.int/eogateway/search">https://earth.esa.int/eogateway/search</a>
SPOT	<a href="https://earth.esa.int/eogateway/missions/spot">https://earth.esa.int/eogateway/missions/spot</a>	<a href="https://earthexplorer.usgs.gov/">https://earthexplorer.usgs.gov/</a> <a href="https://earth.esa.int/eogateway/search">https://earth.esa.int/eogateway/search</a>
SSEBop	<a href="https://www.usgs.gov/data/operational-global-actual-evapotranspiration-using-ssebop-model">https://www.usgs.gov/data/operational-global-actual-evapotranspiration-using-ssebop-model</a>	<a href="https://www.usgs.gov/data/operational-global-actual-evapotranspiration-using-ssebop-model">https://www.usgs.gov/data/operational-global-actual-evapotranspiration-using-ssebop-model</a>
The Climate Hazards Group InfraRed Precipitation with Station Data (CHIRPS)	<a href="https://chg.ucsb.edu/data/chirps">https://chg.ucsb.edu/data/chirps</a>	<a href="https://chg.ucsb.edu/data/chirps">https://chg.ucsb.edu/data/chirps</a>
TRMM	<a href="https://gpm.nasa.gov/missions/trmm">https://gpm.nasa.gov/missions/trmm</a>	<a href="https://gportal.jaxa.jp/gpr/">https://gportal.jaxa.jp/gpr/</a> <a href="https://search.earthdata.nasa.gov/">https://search.earthdata.nasa.gov/</a>
University of Delaware (UDEL)	<a href="https://climate.udel.edu/data/">https://climate.udel.edu/data/</a>	<a href="https://psl.noaa.gov/data/gridded/data.UDel_AirT_Precip.html">https://psl.noaa.gov/data/gridded/data.UDel_AirT_Precip.html</a>
WorldCover	<a href="https://esa-worldcover.org/en">https://esa-worldcover.org/en</a>	<a href="https://esa-worldcover.org/en/data-access">https://esa-worldcover.org/en/data-access</a>

which contain many of the datasets mentioned, for example, including JAXA's "GPortal", NASA's "Earthdata", and USGS's "Earth Explorer". Whilst an attempt has been made to refer readers to the original data source, there may be cases where a secondary data source is cited.

## Acknowledgements

We would like to thank Merlinde Kay, Nevenka Bulovic, Willem Vervoort, and Yi Liu for their helpful discussions on some of the products discussed here. We thank the Editor and three reviewers for their constructive and helpful comments. No datasets were used in the preparation of this paper. Jack Lodge is supported by a UNSW Tuition Fee Scholarship. Fiona Johnson is supported by the UNSW Scientia Program and the ARC Training Centre for Data Analytics for Resources and Environments.

## References

- Abdalla, S., Abdeh Kolahchi, A., Ablain, M., Adusumilli, S., Aich Bhowmick, S., Alou-Font, E., Amarouche, L., Andersen, O.B., Antich, H., Aouf, L., Arbic, B., Armitage, T., Arnault, S., Artana, C., Aulicino, G., Ayoub, N., Badulin, S., Baker, S., Banks, C., Bao, L., Barbetta, S., Barceló-Llull, B., Barlier, F., Basu, S., Bauer-Gottwein, P., Becker, M., Beckley, B., Bellefond, N., Belonenko, T., Benkiran, M., Benkouider, T., Bennartz, R., Benveniste, J., Bercher, N., Berge-Nguyen, M., Bettencourt, J., Blarel, F., Blazquez, A., Blumstein, D., Bonnefond, P., Borde, F., Bouffard, J., Boy, F., Boy, J.-P., Brachet, C., Brasseur, P., Braun, A., Brocca, L., Brockley, D., Brodeau, L., Brown, S., Bruinsma, S., Bulczak, A., Buzzard, S., Cahill, M., Calmant, S., Calzas, M., Camici, S., Cancet, M., Capdeville, H., Carabajal, C.C., Carrere, L., Cazenave, A., Chassignet, E.P., Chauhan, P., Cherchali, S., Chereskin, T., Cheymol, C., Ciani, D., Cipollini, P., Cirillo, F., Cosme, E., Coss, S., Cotroneo, Y., Cotton, D., Couhert, A., Coutin-Faye, S., Crétaux, J.-F., Cyr, F., D'ovidio, F., Darrozes, J., David, C., Dayoub, N., De Staerke, D., Deng, X., Desai, S., Desjonquieres, J.-D., Dettmering, D., Di Bella, A., Díaz-Barroso, L., Dibarboore, G., Dieng, H.B., Dinardo, S., Dobslaw, H., Dodet, G., Doglioli, A., Domeneghetti, A., Donahue, D., Dong, S., Donlon, C., et al., 2021. Altimetry for the future: building on 25 years of progress. *Adv. Space Res.* 68, 319–363.
- Adler, R.F., Sapiano, M.R.P., Huffman, G.J., Wang, J.-J., Gu, G., Bolvin, D., Chiu, L., Schneider, U., Becker, A., Nelkin, E., Xie, P., Ferraro, R., Shin, D.-B., 2018. The Global Precipitation Climatology Project (GPCP) Monthly Analysis (New Version 2.3) and a Review of 2017 Global Precipitation. *Atmosphere* 9, 138.
- Ahamed, T., Tian, L., Zhang, Y., Ting, K.C., 2011. A review of remote sensing methods for biomass feedstock production. *Biomass Bioenergy* 35, 2455–2469.
- Al Zayed, I.S., Elagib, N.A., 2017. Implications of non-sustainable agricultural water policies for the water-food nexus in large-scale irrigation systems: a remote sensing approach. *Adv. Water Resour.* 110, 408–422.
- Alam, S., Gebremichael, M., Li, R., 2019. Remote Sensing-Based Assessment of the Crop, Energy and Water Nexus in the Central Valley, California, 11, p. 1701.
- Alfieri, L., Lorini, V., Hirpa, F.A., Harrigan, S., Zsoter, E., Prudhomme, C., Salamon, P., 2020. A global streamflow reanalysis for 1980–2018. *J. Hydrol. X* 6, 100049.
- Alsdorf, D.E., Rodríguez, E., Lettenmaier, D.P., 2007. Measuring surface water from space. *Rev. Geophys.* 45.
- Altenau, E.H., Pavelsky, T.M., Durand, M.T., Yang, X., Frasson, R.P.D.M., Bendezu, L., 2021. The Surface Water and Ocean Topography (SWOT) Mission River Database (SWORD): a global river network for satellite data products. *Water Resour. Res.* 57 e2021WR030054.
- Angelis-Dimakis, A., Biberacher, M., Dominguez, J., Fiorese, G., Gadocha, S., Gnansounou, E., Guariso, G., Kartalidis, A., Panichelli, L., Pinedo, I., Robba, M., 2011. Methods and tools to evaluate the availability of renewable energy sources. *Renew. Sust. Energ. Rev.* 15, 1182–1200.
- Arun Kumar, S.V.V., Nagababu, G., Sharma, R., Kumar, R., 2020. Synergetic use of multiple scatterometers for offshore wind energy potential assessment. *Ocean Eng.* 196, 106745.
- Ashouri, H., Hsu, K.-L., Sorooshian, S., Braithwaite, D.K., Knapp, K.R., Cecil, L.D., Nelson, B.R., Prat, O.P., 2015. PERSIANN-CDR: daily precipitation climate data record from multisatellite observations for hydrological and climate studies. *Bull. Am. Meteorol. Soc.* 96, 69–83.
- Avtar, R., Sahu, N., Aggarwal, A.K., Chakraborty, S., Kharrazi, A., Yunus, A.P., Dou, J., Kurniawan, T.A., 2019. Exploring renewable energy resources using remote sensing and GIS—a review. *Resources* 8, 149.
- Bach, H., Bird, J., Clausen, T., Jensen, K., Lange, R., Taylor, R., Viriyasakultorn, V., Wolf, A., 2012. Transboundary River Basin Management: Addressing Water, Energy and Food Security. *Mekong River Commission, Lao PDR*.

- Bakhshianlamouki, E., Masia, S., Karimi, P., Van der Zaag, P., Sušnik, J., 2020. A system dynamics model to quantify the impacts of restoration measures on the water-energy-food nexus in the Urmia lake Basin. *Iran. Sci. Total Environ.* 708, 134874.
- Basheer, M., Suliman, R., Ribbe, L., 2021. Exploring management approaches for water and energy in the data-scarce Tekeze-Atbara Basin under hydrologic uncertainty. *Int. J. Water Resour. Dev.* 37, 182–207.
- Bateson, L., Vellico, M., Beaubien, S.E., Pearce, J.M., Annunziatellis, A., Ciotoli, G., Coren, F., Lombardi, S., Marsh, S., 2008. The application of remote-sensing techniques to monitor CO<sub>2</sub>-storage sites for surface leakage: method development and testing at Latera (Italy) where naturally produced CO<sub>2</sub> is leaking to the atmosphere. *Int. J. Greenhouse Gas Control* 2, 388–400.
- Baup, F., Frappart, F., Maubant, J., 2014. Combining high-resolution satellite images and altimetry to estimate the volume of small lakes. *Hydrol. Earth Syst. Sci.* 18, 2007–2020.
- Beck, H.E., Vergopolan, N., Pan, M., Levizzani, V., Van Dijk, A.I.J.M., Weedon, G.P., Brocca, L., Pappenberger, F., Huffman, G.J., Wood, E.F., 2017. Global-scale evaluation of 22 precipitation datasets using gauge observations and hydrological modeling. *Hydrol. Earth Syst. Sci.* 21, 6201–6217.
- Bazilian, M., Rogner, H., Howells, M., Hermann, S., Arent, D., Gielen, D., Steduto, P., Mueller, A., Komor, P., Tol, R.S.J., Yumkella, K.K., 2011. Considering the energy, water and food nexus: Towards an integrated modelling approach. *Energy Policy* 39, 7896–7906.
- Beck, H.E., Pan, M., Roy, T., Weedon, G.P., Pappenberger, F., Van Dijk, A.I.J.M., Huffman, G.J., Adler, R.F., Wood, E.F., 2019a. Daily evaluation of 26 precipitation datasets using Stage-IV gauge-radar data for the CONUS. *Hydrol. Earth Syst. Sci.* 23, 207–224.
- Beck, H.E., Wood, E.F., Pan, M., Fisher, C.K., Miralles, D.G., Van Dijk, A.I.J.M., McVicar, T.R., Adler, R.F., 2019b. MSWEP V2 Global 3-Hourly 0.1° precipitation: methodology and quantitative assessment. *Bull. Am. Meteorol. Soc.* 100, 473–500.
- Becker, M.W., 2006. Potential for satellite remote sensing of ground water. *Groundwater* 44, 306–318.
- Beltran, C.M., Belmonte, A.C., 2001. Irrigated crop area estimation using Landsat TM imagery in La Mancha, Spain. *Photogramm. Eng. Remote. Sens.* 67, 1177–1184.
- Bessho, K., Date, K., Hayashi, M., Ikeda, A., Imai, T., Inoue, H., Kumagai, Y., Miyakawa, T., Murata, H., Ohno, T., Okuyama, A., Oyama, R., Sasaki, Y., Shimazu, Y., Shimoji, K., Sumida, Y., Suzuki, M., Taniguchi, H., Tsuchiyama, H., Uesawa, D., Yokota, H., Yoshida, R., 2016. An introduction to Himawari-8/9—Japan's new-generation geostationary meteorological satellites. *J. Meteorol. Soc. Japan. Ser. II* 94, 151–183.
- Biggs, T.W., Thenkabail, P.S., Gumma, M.K., Scott, C.A., Parthasaradhi, G.R., Turrel, H.N., 2006. Irrigated area mapping in heterogeneous landscapes with MODIS time series, ground truth and census data, Krishna Basin, India. *Int. J. Remote Sens.* 27, 4245–4266.
- Birkett, C., Reynolds, C., Beckley, B., Doorn, B., 2011. From research to operations: the USDA global reservoir and lake monitor. In: Vignudelli, S., Kostianoy, A.G., Cipollini, P., Benveniste, J. (Eds.), *Coastal Altimetry*. Springer Berlin Heidelberg, Berlin, Heidelberg.
- Blanc, P., Gschwind, B., Lefevre, M., Wald, L., 2011. The HelioClim project: surface solar irradiance data for climate applications. *Remote Sens.* 3, 343–361.
- Bonan, G.B., 1996. Land surface model (LSM version 1.0) for ecological, hydrological, and atmospheric studies: Technical description and users guide. Technical note. National Center for Atmospheric Research, Boulder, CO(United States ....).
- Bosilovich, M.G., Chen, J., Robertson, F.R., Adler, R.F., 2008. Evaluation of global precipitation in reanalyses. *J. Appl. Meteorol. Climatol.* 47, 2279–2299.
- Brouwer, C., Heilboem, M., 1985. Irrigation water management: training manual no. 3: irrigation water needs. *Irrigation water management: Training manual no. 3.*
- Brown, M.E., 2016. Remote sensing technology and land use analysis in food security assessment. *J. Land Use Sci.* 11, 623–641.
- Cansino-Loeza, B., Ponce-Ortega, J.M., 2021. Sustainable assessment of Water-Energy-Food Nexus at regional level through a multi-stakeholder optimization approach. *J. Clean. Prod.* 290, 125194.
- Chao, Z., Liu, N., Zhang, P., Ying, T., Song, K., 2019. Estimation methods developing with remote sensing information for energy crop biomass: a comparative review. *Biomass Bioenergy* 122, 414–425.
- Chen, F., Crow, W.T., Bindlish, R., Colliander, A., Burgin, M.S., Asanuma, J., Aida, K., 2018a. Global-scale evaluation of SMAP, SMOS and ASCAT soil moisture products using triple collocation. *Remote Sens. Environ.* 214, 1–13.
- Chen, Y., Lu, D., Luo, L., Pokhrel, Y., Deb, K., Huang, J., Ran, Y., 2018b. Detecting irrigation extent, frequency, and timing in a heterogeneous arid agricultural region using MODIS time series, Landsat imagery, and ancillary data. *Remote Sens. Environ.* 204, 197–211.
- Chen, S., Useya, J., Mugiyono, H., 2020. Decision-level fusion of Sentinel-1 SAR and Landsat 8 OLI texture features for crop discrimination and classification: case of Masvingo, Zimbabwe. *Heliyon* 6, e05358.
- Chen, X., Su, Z., Ma, Y., Trigo, I., Gentile, P., 2021. Remote sensing of global daily evapotranspiration based on a surface energy balance method and reanalysis data. *J. Geophys. Res.-Atmos.* 126 e2020JD032873.
- Claverie, M., Matthews, J.L., Vermote, E.F., Justice, C.O., 2016. A 30+ Year AVHRR LAI and FAPAR climate data record: algorithm description and validation. *Remote Sens.* 8, 263.
- Coolbaugh, M., Kratt, C., Fallacaro, A., Calvin, W., Taranik, J., 2007. Detection of geothermal anomalies using advanced spaceborne thermal emission and reflection radiometer (ASTER) thermal infrared images at Bradys Hot Springs, Nevada, USA. *Remote Sens. Environ.* 106, 350–359.
- Coskun, H.G., Alganci, U., Eris, E., Aguralioglu, N., Cigizoglu, H.K., Yilmaz, L., Toprak, Z., F., 2010. Remote sensing and GIS innovation with hydrologic modelling for Hydroelectric Power Plant (HPP) in poorly gauged basins. *Water Resour. Manag.* 24, 3757–3772.
- Courault, D., Seguin, B., Olioso, A., 2005. Review on estimation of evapotranspiration from remote sensing data: from empirical to numerical modeling approaches. *Irrig. Drain. Syst.* 19, 223–249.
- Crétaux, J.-F., Birkett, C., 2006. Lake studies from satellite radar altimetry. *Compt. Rendus Geosci.* 338, 1098–1112.
- Crétaux, J.-F., Calmant, S., Del Rio, R.A., Kouraev, A., Bergé-Nguyen, M., Maisongrande, P., 2011a. Lakes studies from satellite altimetry. In: Vignudelli, S., Kostianoy, A.G., Cipollini, P., Benveniste, J. (Eds.), *Coastal Altimetry*. Springer Berlin Heidelberg, Berlin, Heidelberg.
- Crétaux, J.-F., Arsen, A., Calmant, S., Kouraev, A., Vuglinski, V., Bergé-Nguyen, M., Gennero, M.C., Nino, F., Abarca Del Rio, R., Cazenave, A., Maisongrande, P., 2011b. SOLS: A lake database to monitor in the Near Real Time water level and storage variations from remote sensing data. *Adv. Space Res.* 47, 1497–1507.
- Crétaux, J.-F., Bergé-Nguyen, M., Calmant, S., Jamangulova, N., Satylkanov, R., Lyard, F., Perosanz, F., Verron, J., Samine Motazem, A., Le Guilcher, G., Leroux, D., Barrie, J., Maisongrande, P., Bonnefond, P., 2018. Absolute calibration or validation of the altimeters on the sentinel-3A and the Jason-3 over Lake Issykkul (Kyrgyzstan). *Remote Sens.* 10, 1679.
- Damiani, A., Irie, H., Horio, T., Takamura, T., Khatri, P., Takenaka, H., Nagao, T., Nakajima, T.Y., Cordero, R.R., 2018. Evaluation of Himawari-8 surface downwelling solar radiation by ground-based measurements. *Atmos. Meas. Tech.* 11, 2501–2521.
- De Strasser, L., Lipponen, A., Howells, M., Stec, S., Bréthaut, C., 2016. A Methodology to Assess the Water Energy Food Ecosystems Nexus in Transboundary River Basins., 8, p. 59.
- Derin, Y., Yilmaz, K.K., 2014. Evaluation of multiple satellite-based precipitation products over complex topography. *J. Hydrometeorol.* 15, 1498–1516.
- Díaz-Alcalde, S., Martínez-Santos, P., 2019. Review: advances in groundwater potential mapping. *Hydrogeol. J.* 27, 2307–2324.
- Didan, K., 2015. MOD13A3 MODIS/Terra vegetation indices monthly L3 global 1km SIN grid V006. NASA EOSDIS LAND PROCESSES DAAC 10.
- Do, H.X., Gudmundsson, L., Leonard, M., Westra, S., 2018. The Global Streamflow Indices and Metadata Archive (GSIM) – Part 1: the production of a daily streamflow archive and metadata. *Earth Syst. Sci. Data* 10, 765–785.
- Doraiswamy, P.C., Hatfield, J.L., Jackson, T.J., Akhmedov, B., Prueger, J., Stern, A., 2004. Crop condition and yield simulations using Landsat and MODIS. *Remote Sens. Environ.* 92, 548–559.
- Doraiswamy, P.C., Sinclair, T.R., Hollinger, S., Akhmedov, B., Stern, A., Prueger, J., 2005. Application of MODIS derived parameters for regional crop yield assessment. *Remote Sens. Environ.* 97, 192–202.
- Dorigo, W., Himmelbauer, I., Aberer, D., Schremmer, L., Petrakovics, I., Zappa, L., Preimesberger, W., Xaver, A., Annor, F., Ardö, J., Baldocchi, D., Bitelli, M., Blöschl, G., Bogena, H., Brocca, L., Calvet, J.C., Camarero, J.J., Capello, G., Choi, M., Cosh, M.C., Van De Giesen, N., Hajdu, I., Ikonen, J., Jensen, K.H., Kanniah, K.D., De Kat, I., Kirchengast, G., Kumar Rai, P., Kyrouac, J., Larson, K., Liu, S., Loew, A., Moghaddam, M., Martínez Fernández, J., Mattar Bader, C., Morbidelli, R., Musial, J. P., Osenga, E., Palecki, M.A., Pellarin, T., Petropoulos, G.P., Pfeil, I., Powers, J., Robock, A., Rüdiger, C., Rummel, U., Strobel, M., Su, Z., Sullivan, R., Tagesson, T., Varlagin, A., Vreugdenhil, M., Walker, J., Wen, J., Wenger, F., Wigneron, J.P., Woods, M., Yang, K., Zeng, Y., Zhang, X., Zreda, M., Dietrich, S., Gruber, A., Van Oevelen, P., Wagner, W., Scipal, K., Drusch, M., Sabia, R., 2021. The International Soil Moisture Network: serving Earth system science for over a decade. *Hydrol. Earth Syst. Sci.* 25, 5749–5804.
- Dörnhöfer, K., Oppelt, N., 2016. Remote sensing for lake research and monitoring – recent advances. *Ecol. Indic.* 64, 105–122.
- Drusch, M., Moreno, J., Bello, U.D., Franco, R., Goulas, Y., Huth, A., Kraft, S., Middleton, E.M., Miglietta, F., Mohammed, G., Nedbal, L., Rascher, U., Schüttmeyer, D., Verhoef, W., 2017. The FLuorescence EXplorer Mission Concept—ESA's Earth Explorer 8. *IEEE Trans. Geosci. Remote Sens.* 55, 1273–1284.
- Duan, Z., Bastiaanssen, W.G.M., 2013. Estimating water volume variations in lakes and reservoirs from four operational satellite altimetry databases and satellite imagery data. *Remote Sens. Environ.* 134, 403–416.
- Duygu, M.B., Akyürek, Z., 2019. Using cosmic-ray neutron probes in validating satellite soil moisture products and land surface models. *Water* 11, 1362.
- Eissa, Y., Korany, M., Aoun, Y., Boraiy, M., Abdel Wahab, M.M., Alfaro, S.C., Blanc, P., El-Metwally, M., Ghedira, H., Hungershoffer, K., Wald, L., 2015. Validation of the surface downwelling solar irradiance estimates of the HelioClim-3 database in Egypt. *Remote Sens.* 7, 9269–9291.
- Elbeih, S.F., 2015. An overview of integrated remote sensing and GIS for groundwater mapping in Egypt. *Ain Shams Eng. J.* 6, 1–15.
- Elewa, H.H., Qaddah, A.A., 2011. Groundwater potentiality mapping in the Sinai Peninsula, Egypt, using remote sensing and GIS-watershed-based modeling. *Hydrogeol. J.* 19, 613–628.
- El-Shirbiny, M.A., Abutaleb, K.A., 2018. Monitoring of water-level fluctuation of Lake Nasser using altimetry satellite data. *Earth Syst. Environ.* 2, 367–375.
- Emery, C.M., Paris, A., Biancamaria, S., Boone, A., Calmant, S., Garambois, P.A., Santos Da Silva, J., 2018. Large-scale hydrological model river storage and discharge correction using a satellite altimetry-based discharge product. *Hydrol. Earth Syst. Sci.* 22, 2135–2162.
- Entekhabi, D., Njoku, E.G., Neill, P.E.O., Kellogg, K.H., Crow, W.T., Edelstein, W.N., Entin, J.K., Goodman, S.D., Jackson, T.J., Johnson, J., Kimball, J., Piepmeyer, J.R., Koster, R.D., Martin, N., McDonald, K.C., Moghaddam, M., Moran, S., Reichle, R., Shi, J.C., Spencer, M.W., Thurman, S.W., Tsang, L., Zyl, J.V., 2010. The Soil Moisture Active Passive (SMAP) mission. *Proc. IEEE* 98, 704–716.

- EROS, 2018. USGS EROS Archive - Land Cover Products - Global Land Cover Characterization (GLCC) Background [Online]. Available: <https://www.usgs.gov/centers/eros/science/usgs-eros-archive-land-cover-products-global-land-cover-characterization-0> [Accessed].
- Eurek, K., Sullivan, P., Gleason, M., Hettinger, D., Heimiller, D., Lopez, A., 2017. An improved global wind resource estimate for integrated assessment models. *Energy Econ.* 64, 552–567.
- Famiglietti, J.S., 2014. The global groundwater crisis. *Nat. Clim. Chang.* 4, 945–948.
- Fan, W., Liu, Y., Chappell, A., Dong, L., Xu, R., Ekström, M., Fu, T.-M., Zeng, Z., 2021. Evaluation of global reanalysis land surface wind speed trends to support wind energy development using in situ observations. *J. Appl. Meteorol. Climatol.* 60, 33–50.
- Fan, J., Han, Q., Tan, S., Li, J., 2022. Evaluation of six satellite-based soil moisture products based on in situ measurements in Hunan Province, Central China. *Front. Environ. Sci.* 10.
- Fang, L., Hain, C.R., Zhan, X., Anderson, M.C., 2016. An inter-comparison of soil moisture data products from satellite remote sensing and a land surface model. *Int. J. Appl. Earth Obs. Geoinf.* 48, 37–50.
- Fang, H., Baret, F., Plummer, S., Schaepman-Strub, G., 2019. An overview of Global Leaf Area Index (LAI): methods, products, validation, and applications. *Rev. Geophys.* 57, 739–799.
- FAO, 2014. The Water-Energy-Food Nexus A new approach in support of food security and sustainable agriculture. Rome.
- Faticchi, S., Vivoni, E., Ogden, F., Ivanov, V., Mirus, B., Gochis, D., Downer, C., Camporese, M., Davison, J., Ebel, B., Jones, N., Kim, J., Mascaro, G., Niswonger, R., Restrepo, P., Rigon, R., Shen, C., Sulis, M., Tarboton, D., 2016. An overview of current applications, challenges, and future trends in distributed process-based models in hydrology. *J. Hydrol.* 537.
- Fisher, R.A., Koven, C.D., 2020. Perspectives on the future of land surface models and the challenges of representing complex terrestrial systems. *J. Adv. Model. Earth Syst.* 12 e2018MS001453.
- Fisher, J.B., Lee, B., Purdy, A.J., Halverson, G.H., Dohlen, M.B., Cawse-Nicholson, K., Wang, A., Anderson, R.G., Aragon, B., Arain, M.A., 2020. ECOSTRESS: NASA's next generation mission to measure evapotranspiration from the international space station. *Water Resour. Res.* 56 e2019WR026058.
- Frappart, F., Ramilien, G., 2018. Monitoring Groundwater Storage Changes Using the Gravity Recovery and Climate Experiment (GRACE) satellite mission: a review. *Remote Sens.* 10, 829.
- Funk, C., Peterson, P., Landsfeld, M., Pedreros, D., Verdin, J., Shukla, S., Husak, G., Rowland, J., Harrison, L., Hoell, A., Michaelsen, J., 2015. The climate hazards infrared precipitation with stations—a new environmental record for monitoring extremes. *Sci. Data* 2, 150066.
- Gao, H., 2015. Satellite remote sensing of large lakes and reservoirs: from elevation and area to storage. *WIREs Water* 2, 147–157.
- Gao, J., Zhang, A., Lam, S.K., Zhang, X., Thomson, A.M., Lin, E., Jiang, K., Clarke, L.E., Edmonds, J.A., Kyle, P.G., Yu, S., Zhou, Y., Zhou, S., 2016. An integrated assessment of the potential of agricultural and forestry residues for energy production in China. *GCB Bioenergy* 8, 880–893.
- Gararo, R., McCarty, W., Suárez, M.J., Todling, R., Molod, A., Takacs, L., Randles, C.A., Darmenov, A., Bosilovich, M.G., Reichle, R., Wargin, K., Coy, L., Cullather, R., Draper, C., Akella, S., Buchard, V., Conaty, A., Da Silva, A.M., Gu, W., Kim, G.-K., Koster, R., Lucchesi, R., Merkova, D., Nielsen, J.E., Partyka, G., Pawson, S., Putman, W., Rienecker, M., Schubert, S.D., Sienkiewicz, M., Zhao, B., 2017. The modern-era retrospective analysis for research and applications, Version 2 (MERRA-2). *J. Clim.* 30, 5419–5454.
- Ghiggi, G., Humphrey, V., Seneviratne, S.I., Gudmundsson, L., 2021. G-RUN ENSEMBLE: a multi-forcing observation-based global runoff reanalysis. *Water Resour. Res.* 57 e2020WR028787.
- Gleason, C.J., Durand, M.T., 2020. Remote sensing of river discharge: a review and a framing for the discipline. *Remote Sens.* 12, 1107.
- Global Solar Atlas, 2019a. *Global Solar Atlas 2.0* [Online]. Solargis. Available: <https://globalsolaratlas.info/> [Accessed 02 March 2022].
- Global Solar Atlas, 2019b. *Global Solar Atlas 2.0 | Accuracy* [Online]. Available: <https://globalsolaratlas.info/support/accuracy> [Accessed 02 March 2022].
- Gomis-Cebolla, J., Jimenez, J.C., Sobrino, J.A., Corbari, C., Mancini, M., 2019. Intercomparison of remote-sensing-based evapotranspiration algorithms over amazonian forests. *Int. J. Appl. Earth Obs. Geoinf.* 80, 280–294.
- Gonçalves, A.C., Malico, I., Sousa, A.M., 2021. Energy production from forest biomass: An overview. *Forest Biomass-From Trees to Energy*.
- Grippa, M., Rouzies, C., Biancamaria, S., Blumstein, D., Creteaux, J.F., Gal, L., Robert, E., Gosset, M., Kergoat, L., 2019. Potential of SWOT for monitoring water volumes in Sahelian ponds and lakes. *IEEE J. Select. Top. Appl. Earth Observ. Remote Sens.* 12, 2541–2549.
- Gruber, A., Scanlon, T., Van Der Schalie, R., Wagner, W., Dorigo, W., 2019. Evolution of the ESA CCI Soil Moisture climate data records and their underlying merging methodology. *Earth Syst. Sci. Data* 11, 717–739.
- Gruber, K., Regner, P., Wehrle, S., Zeyringer, M., Schmidt, J., 2022. Towards global validation of wind power simulations: a multi-country assessment of wind power simulation from MERRA-2 and ERA-5 reanalyses bias-corrected with the global wind atlas. *Energy* 238, 121520.
- Gualtieri, G., 2022. Analysing the uncertainties of reanalysis data used for wind resource assessment: A critical review. *Renew. Sust. Energ. Rev.* 167, 112741.
- Guan, K., Berry, J.A., Zhang, Y., Joiner, J., Gualtieri, L., Badgley, G., Lobell, D.B., 2016. Improving the monitoring of crop productivity using spaceborne solar-induced fluorescence. *Glob. Chang. Biol.* 22, 716–726.
- Guan, K., Wu, J., Kimball, J.S., Anderson, M.C., Frolking, S., Li, B., Hain, C.R., Lobell, D.B., 2017. The shared and unique values of optical, fluorescence, thermal and microwave satellite data for estimating large-scale crop yields. *Remote Sens. Environ.* 199, 333–349.
- Guerschman, J.P., McVicar, T.R., Vleeshouwer, J., Van Niel, T.G., Peña-Arancibia, J.L., Chen, Y., 2022. Estimating actual evapotranspiration at field-to-continent scales by calibrating the CMRSET algorithm with MODIS, VIIRS, Landsat and Sentinel-2 data. *J. Hydrol.* 605, 127318.
- Guimaraes, N., Godinho, S., Rivera, M., Pinto-Correia, T., Machado, R., Czekaj, M., Tyran, E., Puchala, J., 2021. Assessing food availability: a novel approach for the quantitative estimation of the contribution of small farms in regional food systems in Europe. *Glob. Food Secur.* 30, 10055.
- Hammer, A., Heinemann, D., Lorenz, E., Lückehe, B., 1999. Short-term forecasting of solar radiation: a statistical approach using satellite data. *Sol. Energy* 67, 139–150.
- Hammer, A., Heinemann, D., Hoyer, C., Kuhlemann, R., Lorenz, E., Müller, R., Beyer, H.G., 2003. Solar energy assessment using remote sensing technologies. *Remote Sens. Environ.* 86, 423–432.
- Han, J.-Y., Vohnicky, P., 2022. An optimized approach for mapping solar irradiance in a mid-low latitude region based on a site-adaptation technique using Himawari-8 satellite imageries. *Renew. Energy* 187, 603–617.
- Harrigan, S., Szoter, E., Alfieri, L., Prudhomme, C., Salamon, P., Wetterhall, F., Barnard, C., Cloke, H., Pappenberger, F., 2020. GloFAS-ERA5 operational global river discharge reanalysis 1979–present. *Earth Syst. Sci. Data* 12, 2043–2060.
- Hasager, C.B., Pena, A., Christiansen, M.B., Astrup, P., Nielsen, M., Monaldo, F., Thompson, D., Nielsen, P., 2008. Remote sensing observation used in offshore wind energy. *IEEE J. Select. Top. Appl. Earth Observ. Remote Sens.* 1, 67–79.
- Haselwimmer, C., Prakash, A., 2013. Thermal Infrared Remote Sensing of geoTHERMAL systems. *Thermal Infrared Remote Sensing*. Springer.
- Heasler, H., Jaworowski, C., 2018. Hydrothermal monitoring of Norris Geyser Basin, Yellowstone National Park, USA, using airborne thermal infrared imagery. *Geothermics* 72, 24–46.
- Hersbach, H., Bell, B., Berrisford, P., Hirahara, S., Horányi, A., Muñoz-Sabater, J., Nicolas, J., Peubey, C., Radu, R., Schepers, D., Simmons, A., Soci, C., Abdalla, S., Abellán, X., Balsamo, G., Bechtold, P., Biavati, G., Bidlot, J., Bonavita, M., De Chiara, G., Dahlgren, P., Dee, D., Diamantakis, M., Dragani, R., Flemming, J., Forbes, R., Fuentes, M., Geer, A., Haimberger, L., Healy, S., Hogan, R.J., Hölm, E., Janisková, M., Keeley, S., Laloyaux, P., Lopez, P., Lupu, C., Radnoti, G., De Rosnay, P., Rozum, I., Vamborg, F., Villaume, S., Thépaut, J.-N., 2020. The ERA5 global reanalysis. *Q. J. R. Meteorol. Soc.* 146, 1999–2049.
- Hiloidhari, M., Das, D., Baruah, D.C., 2014. Bioenergy potential from crop residue biomass in India. *Renew. Sust. Energ. Rev.* 32, 504–512.
- Hirooka, D., Murata, N., Fujimoto, Y., Hayashi, Y., 2018. Temporal interpolation of gridded solar radiation data for evaluation of PV fluctuations. *Energy Procedia* 155, 259–268.
- Hu, Z., Hu, Q., Zhang, C., Chen, X., Li, Q., 2016. Evaluation of reanalysis, spatially interpolated and satellite remotely sensed precipitation data sets in central Asia. *J. Geophys. Res.-Atmos.* 121, 5648–5663.
- Huang, G., Li, Z., Li, X., Liang, S., Yang, K., Wang, D., Zhang, Y., 2019. Estimating surface solar irradiance from satellites: past, present, and future perspectives. *Remote Sens. Environ.* 233, 111371.
- Huang, Q., Qin, G., Zhang, Y., Tang, Q., Liu, C., Xia, J., Chiew, F.H.S., Post, D., 2020. Using remote sensing data-based hydrological model calibrations for predicting runoff in ungauged or poorly gauged catchments. *56 e2020WR028205*.
- Huffman, G.J., Adler, R.F., Bolvin, D.T., Nelkin, E.J., 2010. The TRMM Multi-Satellite Precipitation Analysis (TMPA). In: Gebremichael, M., Hossain, F. (Eds.), *Satellite Rainfall Applications for Surface Hydrology*. Springer Netherlands, Dordrecht.
- Huffman, G.J., Bolvin, D.T., Braithwaite, D., Hsu, K., Joyce, R., Xie, P., Yoo, S.-H., 2015. NASA global precipitation measurement (GPM) integrated multi-satellite retrievals for GPM (IMERG). *Algorithm Theoretical Basis Document (ATBD)* Version 4, 26.
- Huffman, G.J., Bolvin, D.T., Braithwaite, D., Hsu, K.-L., Joyce, R.J., Kidd, C., Nelkin, E.J., Sorooshian, S., Stocker, E.F., Tan, J., Wolff, D.B., Xie, P., 2020. Integrated Multi-satellite Retrievals for the Global Precipitation Measurement (GPM) Mission (IMERG). In: Levizzani, V., Kidd, C., Kirschbaum, D.B., Kummerow, C.D., Nakamura, K., Turk, F.J. (Eds.), *Satellite Precipitation Measurement*, Vol. 1. Springer International Publishing, Cham.
- IEA, 2019. Offshore Wind Outlook 2019.
- IEA, 2021. *Renewable Power* [Online]. IEA, Paris. Available: <https://www.iea.org/reports/renewable-power> [Accessed].
- Jackson, T.J., 2002. Remote sensing of soil moisture: implications for groundwater recharge. *Hydrogeol. J.* 10, 40–51.
- Jaiswal, R.K., Ali, S., Bharti, B., 2020. Comparative evaluation of conceptual and physical rainfall-runoff models. *Appl. Water Sci.* 10, 48.
- Jalilov, S.-M., Varis, O., Keskinen, M., 2015. Sharing Benefits in Transboundary Rivers: An Experimental Case Study of Central Asian Water-Energy-Agriculture Nexus, 7, pp. 4778–4805.
- Jha, M.K., Chowdhury, A., Chowdary, V.M., Peiffer, S., 2007. Groundwater management and development by integrated remote sensing and geographic information systems: prospects and constraints. *Water Resour. Manag.* 21, 427–467.
- Ji, L., Zhang, L., Wylie, B.K., 2009. Analysis of dynamic thresholds for the normalized difference water index. *Photogramm. Eng. Remote. Sens.* 75, 1307–1317.
- Jia, K., Li, Q., Tian, Y., Wu, B., Zhang, F., Meng, J., 2012. Crop classification using multi-configuration SAR data in the North China Plain. *Int. J. Remote Sens.* 33, 170–183.
- Jia, D., Hua, J., Wang, L., Guo, Y., Guo, H., Wu, P., Liu, M., Yang, L., 2021. Estimations of global horizontal irradiance and direct normal irradiance by using fengyun-4A satellite data in Northern China. *Remote Sens.* 13, 790.

- Jiang, Y., Havrysh, V., Klymchuk, O., Nitsenko, V., Balezentis, T., Streimikiene, D., 2019. Utilization of crop residue for power generation: the case of Ukraine. *Sustainability* 11, 7004.
- Jódar, J., Carpintero, E., Martos-Rosillo, S., Ruiz-Constán, A., Marín-Lechado, C., Cabrera-Arrabal, J.A., Navarrete-Mazriegos, E., González-Ramón, A., Lambán, L.J., Herrera, C., González-Dugo, M.P., 2018. Combination of lumped hydrological and remote-sensing models to evaluate water resources in a semi-arid high altitude ungauged watershed of Sierra Nevada (Southern Spain). *Sci. Total Environ.* 625, 285–300.
- Jourdier, B., 2020. Evaluation of ERA5, MERRA-2, COSMO-REA6, NEWA and AROME to simulate wind power production over France. *Adv. Sci. Res.* 17, 63–77.
- Jun, C., Ban, Y., Li, S., 2014. Open access to Earth land-cover map. *Nature* 514, 434.
- Kaddoura, S., El Khatib, S., 2017. Review of water-energy-food Nexus tools to improve the Nexus modelling approach for integrated policy making. *Environ. Sci. Pol.* 77, 114–121.
- Karthikeyan, L., Chawla, I., Mishra, A.K., 2020. A review of remote sensing applications in agriculture for food security: Crop growth and yield, irrigation, and crop losses. *J. Hydrol.* 586, 124905.
- Kenduiwy, B.K., Bargiel, D., Soergel, U., 2018. Crop-type mapping from a sequence of Sentinel 1 images. *Int. J. Remote Sens.* 39, 6383–6404.
- Keskinen, M., Guillaume, J.H.A., Kattelus, M., Porkka, M., Räsänen, T.A., Varis, O., 2016. The water-energy-food nexus and the transboundary context: insights from large Asian rivers. *Water* 8.
- Keyhani, A., Ghasemi-Varnamkhasti, M., Khanali, M., Abbaszadeh, R., 2010. An assessment of wind energy potential as a power generation source in the capital of Iran, Tehran. *Energy* 35, 188–201.
- Kidd, C., Huffman, G., 2011. Global precipitation measurement. *Meteorol. Appl.* 18, 334–353.
- Kim, Y., Jackson, T., Bindlish, R., Lee, H., Hong, S., 2012. Radar vegetation index for estimating the vegetation water content of rice and soybean. *IEEE Geosci. Remote Sens. Lett.* 9, 564–568.
- Kim, H.-G., Kim, J.-Y., Kang, Y.-H., 2018. Comparative evaluation of the third-generation reanalysis data for wind resource assessment of the southwestern offshore in South Korea. *Atmosphere* 9, 73.
- Kim, H., Wigneron, J.-P., Kumar, S., Dong, J., Wagner, W., Cosh, M.H., Bosch, D.D., Collins, C.H., Starks, P.J., Seyfried, M., Lakshmi, V., 2020. Global scale error assessments of soil moisture estimates from microwave-based active and passive satellites and land surface models over forest and mixed irrigated/dryland agriculture regions. *Remote Sens. Environ.* 251, 112052.
- Kira, O., Ngui-Robertson, A.L., Arkebauer, T.J., Linker, R., Gitelson, A.A., 2016. Informative spectral bands for remote green LAI estimation in C3 and C4 crops. *Agric. For. Meteorol.* 218–219, 243–249.
- Kobayashi, S., Ota, Y., Harada, Y., Ebata, A., Moriya, M., Onoda, H., Onogi, K., Kamahori, H., Kobayashi, C., Endo, H., Miyaoka, K., Takahashi, K., 2015. The JRA-55 Reanalysis: general specifications and basic characteristics. *J. Meteorol. Soc. Japan. Ser. II* 93, 5–48.
- Kratt, C., Calvin, W.M., Coolbaugh, M.F., 2010. Mineral mapping in the Pyramid Lake basin: hydrothermal alteration, chemical precipitates and geothermal energy potential. *Remote Sens. Environ.* 114, 2297–2304.
- Kumar, L., Mutanga, O., 2017. Remote sensing of above-ground biomass. *Remote Sens.* 9, 935.
- Kumar, L., Sinha, P., Taylor, S., Alqurashi, F.A., 2015. Review of the use of remote sensing for biomass estimation to support renewable energy generation. *J. Appl. Remote. Sens.* 9, 1–28.
- Kumar, S.V., Dirmeyer, P.A., Peters-Lidard, C.D., Bindlish, R., Bolten, J., 2018. Information theoretic evaluation of satellite soil moisture retrievals. *Remote Sens. Environ.* 204, 392–400.
- Kusre, B.C., Baruah, D.C., Bordoloi, P.K., Patra, S.C., 2010. Assessment of hydropower potential using GIS and hydrological modeling technique in Kopili River basin in Assam (India). *Appl. Energy* 87, 298–309.
- L'Ecuyer, T.S., Beaudoin, H.K., Rodell, M., Olson, W., Lin, B., Kato, S., Clayton, C.A., Wood, E., Sheffield, J., Adler, R., Huffman, G., Bosilovich, M., Gu, G., Robertson, F., Houser, P.R., Chambers, D., Famiglietti, J.S., Fetzer, E., Liu, W.T., Gao, X., Schlosser, C.A., Clark, E., Lettenmaier, D.P., Hilburn, K., 2015. The observed state of the energy budget in the early twenty-first century. *J. Clim.* 28, 8319–8346.
- Labus, M.P., Nielsen, G.A., Lawrence, R.L., Engel, R., Long, D.S., 2002. Wheat yield estimates using multi-temporal NDVI satellite imagery. *Int. J. Remote Sens.* 23, 4169–4180.
- Lai, Y.R., Pringle, M.J., Kopittke, P.M., Menzies, N.W., Orton, T.G., Dang, Y.P., 2018. An empirical model for prediction of wheat yield, using time-integrated Landsat NDVI. *Int. J. Appl. Earth Geoinf.* 72, 99–108.
- Larentis, D.G., Collischonn, W., Olivera, F., Tucci, C.E.M., 2010. Gis-based procedures for hydropower potential spotting. *Energy* 35, 4237–4243.
- Largeron, C., Dumont, M., Morin, S., Boone, A., Lafayesse, M., Metref, S., Cosme, E., Jonas, T., Winstral, A., Margulis, S.A., 2020. Toward snow cover estimation in mountainous areas using modern data assimilation methods: a review. *Front. Earth Sci.* 8.
- Lawston, P.M., Santanello Jr., J.A., Kumar, S.V., 2017. Irrigation signals detected from SMAP soil moisture retrievals. *Geophys. Res. Lett.* 44, 11,860–11,867.
- Lechner, B., Döll, P., 2004. Development and validation of a global database of lakes, reservoirs and wetlands. *J. Hydrol.* 296, 1–22.
- Lettenmaier, D.P., Alsdorf, D., Dozier, J., Huffman, G.J., Pan, M., Wood, E.F., 2015. Inroads of remote sensing into hydrologic science during the WRR era. *Water Resour. Res.* 51, 7309–7342.
- Levizzani, V., Cattani, E., 2019. Satellite remote sensing of precipitation and the terrestrial water cycle in a changing climate. *Remote Sens.* 11, 2301.
- Li, Z.-L., Tang, R., Wan, Z., Bi, Y., Zhou, C., Tang, B., Yan, G., Zhang, X., 2009. A review of current methodologies for regional evapotranspiration estimation from remotely sensed data. *Sensors* 9, 3801–3853.
- Li, B., Rodell, M., Kumar, S., Beaudoin, H.K., Getirana, A., Zaichick, B.F., De Goncalves, L.G., Cossetin, C., Bhajna, S., Mukherjee, A., Tian, S., Tangdamrongsub, N., Long, D., Nanteza, J., Lee, J., Policelli, F., Goni, I.B., Daira, D., Bila, M., De Lannoy, G., Mocko, D., Steele-Dunne, S.C., Save, H., Bettadpur, S., 2019. Global GRACE data assimilation for groundwater and drought monitoring: advances and challenges. *Water Resour. Res.* 55, 7564–7586.
- Li, L., Liu, Y., Zhu, Q., Liao, K., Lai, X., 2022. Evaluation of nine major satellite soil moisture products in a typical subtropical monsoon region with complex land surface characteristics. *Int. Soil Water Conserv. Res.* 10, 518–529.
- Lievens, H., Demuzere, M., Marshall, H.-P., Reichle, R.H., Brucker, L., Brangers, I., De Rosnay, P., Dumont, M., Girotto, M., Immerzeel, W.W., Jonas, T., Kim, E.J., Koch, I., Marty, C., Saloranta, T., Schöberl, J., De Lannoy, G.J.M., 2019. Snow depth variability in the Northern Hemisphere mountains observed from space. *Nat. Commun.* 10, 4629.
- Lillesand, T., Kiefer, R.W., Chipman, J., 2015. *Remote Sensing and Image Interpretation*. John Wiley & Sons.
- Lin, P., Pan, M., Beck, H.E., Yang, Y., Yamazaki, D., Frasson, R., David, C.H., Durand, M., Pavelsky, T.M., Allen, G.H., Gleason, C.J., Wood, E.F., 2019. Global reconstruction of naturalized river flows at 2.94 million reaches. *Water Resour. Res.* 55, 6499–6516.
- Liu, W., Hong, Y., Khan, S., Huang, M., Vieux, B., Caliskan, S., Grout, T., 2010. Actual evapotranspiration estimation for different land use and land cover in urban regions using Landsat 5 data. *J. Appl. Remote. Sens.* 4, 041873.
- Liu, J., Yang, H., Cudennec, C., Gain, A.K., Hoff, H., Lawford, R., Qi, J., Strasser, L.D., Yillia, P.T., Zheng, C., 2017. Challenges in operationalizing the water–energy–food nexus. *Hydrol. Sci. J.* 62, 1714–1720.
- Lopes, F.M., Silva, H.G., Salgado, R., Cavaco, A., Canhoto, P., Collares-Pereira, M., 2018. Short-term forecasts of GHI and DNI for solar energy systems operation: assessment of the ECMWF integrated forecasting system in southern Portugal. *Sol. Energy* 170, 14–30.
- Lu, D., 2006. The potential and challenge of remote sensing-based biomass estimation. *Int. J. Remote Sens.* 27, 1297–1328.
- Lu, S., Ouyang, N., Wu, B., Wei, Y., Tesemma, Z., 2013. Lake water volume calculation with time series remote-sensing images. *Int. J. Remote Sens.* 34, 7962–7973.
- Lund, J.W., Bjelm, L., Bloomquist, G., Mortensen, A.K., 2008. Characteristics, development and utilization of geothermal resources—a Nordic perspective. *Episodes* 31, 140–147.
- Ma, H., Liang, S., 2022. Development of the GLASS 250-m leaf area index product (version 6) from MODIS data using the bidirectional LSTM deep learning model. *Remote Sens. Environ.* 273, 112985.
- Martens, B., Miralles, D.G., Lievens, H., Van Der Schalie, R., De Jeu, R.A.M., Fernández-Prieto, D., Beck, H.E., Dorigo, W.A., Verhoest, N.E.C., 2017. GLEAM v3: satellite-based land evaporation and root-zone soil moisture. *Geosci. Model Dev.* 10, 1903–1925.
- Massari, C., Crow, W., Brocca, L., 2017. An assessment of the performance of global rainfall estimates without ground-based observations. *Hydrol. Earth Syst. Sci.* 21, 4347–4361.
- Massari, C., Modanesi, S., Dari, J., Gruber, A., De Lannoy, G.J.M., Girotto, M., Quintana-Seguí, P., Le Page, M., Jarlan, L., Zribi, M., Ouadi, N., Vreugdenhil, M., Zappa, L., Dorigo, W., Wagner, W., Brombacher, J., Pelgrum, H., Jaquot, P., Freeman, V., Volden, E., Fernandez Prieto, D., Tarpanelli, A., Barbetta, S., Brocca, L., 2021. A review of irrigation information retrievals from space and their utility for users. *Remote Sens.* 13, 4112.
- Matsuura, K., Willmott, C.J., 2018. Terrestrial Air Temperature: 1900–2017 Gridded Monthly Time Series.
- McMahon, T.A., Peel, M.C., Lowe, L., Srikanthan, R., McVicar, T.R., 2013. Estimating actual, potential, reference crop and pan evaporation using standard meteorological data: a pragmatic synthesis. *Hydrol. Earth Syst. Sci.* 17, 1331–1363.
- McNairn, H., Shang, J., 2016. A Review of Multitemporal Synthetic Aperture Radar (SAR) for crop monitoring. In: Ban, Y. (Ed.), *Multitemporal Remote Sensing: Methods and Applications*. Springer International Publishing, Cham.
- McNairn, H., Kross, A., Lapen, D., Caves, R., Shang, J., 2014. Early season monitoring of corn and soybeans with TerraSAR-X and RADARSAT-2. *Int. J. Appl. Earth Obs. Geoinf.* 28, 252–259.
- McVicar, T., Vleeshouwer, J., Van Niel, T., Guerschman, J., 2022. Actual evapotranspiration for Australia using CMRSET algorithm. In: *Terrestrial Ecosystem Research Network* (ed.).
- Miao, H., Dong, D., Huang, G., Hu, K., Tian, Q., Gong, Y., 2020. Evaluation of Northern Hemisphere surface wind speed and wind power density in multiple reanalysis datasets. *Energy* 200, 117382.
- Michaelides, S., Levizzani, V., Anagnostou, E., Bauer, P., Kasparis, T., Lane, J.E., 2009. Precipitation: measurement, remote sensing, climatology and modeling. *Atmos. Res.* 94, 512–533.
- Milly, P.C.D., Betancourt, J., Falkenmark, M., Hirsch, R.M., Kundzewicz, Z.W., Lettenmaier, D.P., Stouffer, R.J., 2008. Stationarity is dead: whither water management? *Science* 319, 573–574.
- Mirasi, A., Mahmoudi, A., Navid, H., Valizadeh Kamran, K., Asoodar, M.A., 2021. Evaluation of sum-NDVI values to estimate wheat grain yields using multi-temporal Landsat OLI data. *Geocarto Int.* 36, 1309–1324.
- Mohammed, G.H., Colombo, R., Middleton, E.M., Rascher, U., Van Der Tol, C., Nedbal, L., Goulas, Y., Pérez-Priego, O., Damm, A., Meroni, M., Joiner, J., Cogliati, S., Verhoeft, W., Malenovský, Z., Gastellu-Etchegorry, J.-P., Miller, J.R., Guanter, L., Moreno, J., Moya, I., Berry, J.A., Frankenberger, C., Zarco-Tejada, P.J.,

2019. Remote sensing of solar-induced chlorophyll fluorescence (SIF) in vegetation: 50 years of progress. *Remote Sens. Environ.* 231, 111177.
- Mohsen, A., Elshemy, M., Zeidan, B.A., 2018. Change detection for Lake Burullus, Egypt using remote sensing and GIS approaches. *Environ. Sci. Pollut. Res.* 25, 30763–30771.
- Mokhtari, A., Noory, H., Vazifedoust, M., 2018. Improving crop yield estimation by assimilating LAI and inputting satellite-based surface incoming solar radiation into SWAT model. *Agric. For. Meteorol.* 250–251, 159–170.
- Monaldo, F.M., Thompson, D.R., Beal, R.C., Pichel, W.G., Clemente-Colon, P., 2001. Comparison of SAR-derived wind speed with model predictions and ocean buoy measurements. *IEEE Trans. Geosci. Remote Sens.* 39, 2587–2600.
- Mongillo, M., Cochane, G., Browne, P., Deroin, J., 1995. Application of satellite imagery to explore and monitor geothermal systems. *Proceed. World Geoth. Congress* 951–956.
- Montzka, C., Bogena, H.R., Zreda, M., Monerris, A., Morrison, R., Muddu, S., Vereecken, H., 2017. Validation of spaceborne and modelled surface soil moisture products with cosmic-ray neutron probes. *Remote Sens.* 9.
- Mu, Q., Zhao, M., Running, S.W., 2011. Improvements to a MODIS global terrestrial evapotranspiration algorithm. *Remote Sens. Environ.* 115, 1781–1800.
- Mulla, D.J., 2013. Twenty five years of remote sensing in precision agriculture: key advances and remaining knowledge gaps. *Biosyst. Eng.* 114, 358–371.
- Müller, R., Pfeifroth, U., Träger-Chatterjee, C., Trentmann, J., Cremer, R., 2015. Digging the METEOSAT treasure—3 decades of solar surface radiation. *Remote Sens.* 7, 8067–8101.
- Muñoz-Sabater, J., Dutra, E., Agustín-Panareda, A., Albergel, C., Arduini, G., Balsamo, G., Boussetta, S., Choulga, M., Harrigan, S., Hersbach, H., Martens, B., Miralles, D.G., Piles, M., Rodríguez-Fernández, N.J., Zsoter, E., Buontempo, C., Thépaut, J.N., 2021. ERA5-Land: a state-of-the-art global reanalysis dataset for land applications. *Earth Syst. Sci. Data* 13, 4349–4383.
- Murthy, K.S.R., Rahi, O.P., 2017. A comprehensive review of wind resource assessment. *Renew. Sust. Energ. Rev.* 72, 1320–1342.
- Musa, Z.N., Popescu, I., Mynett, A., 2015. A review of applications of satellite SAR, optical, altimetry and DEM data for surface water modelling, mapping and parameter estimation. *Hydrol. Earth Syst. Sci.* 19, 3755–3769.
- Mutanga, O., Dube, T., Galal, O., 2017. Remote sensing of crop health for food security in Africa: Potentials and constraints. *Remote Sens. Appl. Soc. Environ.* 8, 231–239.
- Nair, A.S., Kumar, N., Indu, J., Vivek, B., 2021. Monitoring lake levels from space: preliminary analysis with SWOT. *Front. Water* 161.
- NASA, 2020. *SWOT River Products* [Online]. Available: <https://swot.jpl.nasa.gov/resources/136/swot-river-products/> [Accessed 10 July 2022].
- Nicolai-Shaw, N., Hirschi, M., Mittelbach, H., Seneviratne, S.I., 2015. Spatial representativeness of soil moisture using in situ, remote sensing, and land reanalysis data. *J. Geophys. Res.-Atmos.* 120, 9955–9964.
- Njoku, E.G., Jackson, T.J., Lakshmi, V., Chan, T.K., Nghiem, S.V., 2003. Soil moisture retrieval from AmSR-E. *IEEE Trans. Geosci. Remote Sens.* 41, 215–229.
- Nouri, M., Homaei, M., 2022. Future crop evapotranspiration for data-sparse regions using reanalysis products. *Agric. Water Manag.* 262, 107319.
- Oikonomidis, D., Dimogianni, S., Kazakis, N., Voudouris, K., 2015. A GIS/Remote Sensing-based methodology for groundwater potentiality assessment in Tirnavos area, Greece. *J. Hydrol.* 525, 197–208.
- Okamoto, K.I., Ushio, T., Iguchi, T., Takahashi, N., Iwanami, K., 2005. The global satellite mapping of precipitation (GSMaP) project. In: Proceedings. 2005 IEEE International Geoscience and Remote Sensing Symposium, 2005. IGARSS '05, 29–29 July 2005, pp. 3414–3416.
- Olyphant, A., Thenkabail, P., Teluguntla, P., 2022. Global food-security-support-analysis data at 30-m resolution (GFSAD30) cropland-extent products—Download Analysis. Open-File Report, Reston VA.
- OpenET, 2021. *OpenET* [Online]. Available: <https://openetdata.org/> [Accessed 18 May 2022].
- Ozdogan, M., Woodcock, C.E., Salvucci, G.D., Demir, H., 2006. Changes in summer irrigated crop area and water use in Southeastern Turkey from 1993 to 2002: implications for current and future water resources. *Water Resour. Manag.* 20, 467–488.
- Pahl-Wostl, C., 2019. Governance of the water-energy-food security nexus: a multi-level coordination challenge. *Environ. Sci. Pol.* 92, 356–367.
- Palerme, C., Claud, C., Dufour, A., Genthon, C., Wood, N.B., L'Ecuyer, T., 2017. Evaluation of Antarctic snowfall in global meteorological reanalyses. *Atmos. Res.* 190, 104–112.
- Pandey, A., Lalrempuia, D., Jain, S.K., 2015. Assessment of hydropower potential using spatial technology and SWAT modelling in the Mat River, southern Mizoram, India. *Hydrol. Sci. J.* 60, 1651–1665.
- Papa, F., Bala, S.K., Pandey, R.K., Durand, F., Gopalakrishna, V., Rahman, A., Rossow, W.B., 2012. Ganga-Brahmaputra river discharge from Jason-2 radar altimetry: an update to the long-term satellite-derived estimates of continental freshwater forcing flux into the Bay of Bengal. *J. Geophys. Res. Oceans* 117.
- Peña-Arancibia, J.L., Ahmad, M.-U.-D., 2020. Early twenty-first century satellite-driven irrigation performance in the world's largest system: Pakistan's Indus Basin irrigated system. *Environ. Res. Lett.* 16, 014037.
- Peng, B., Guan, K., Zhou, W., Jiang, C., Frankenberger, C., Sun, Y., He, L., Köhler, P., 2020. Assessing the benefit of satellite-based Solar-Induced Chlorophyll Fluorescence in crop yield prediction. *Int. J. Appl. Earth Obs. Geoinf.* 90, 102126.
- Pfeifroth, U., Kothe, S., Trentmann, J., Hollmann, R., Fuchs, P., Kaiser, J., Werscheck, M., 2019. Surface Radiation Data Set - Heliosat (SARAH) - Edition 2.1, Satellite Application Facility on Climate Monitoring.
- Pham, H.T., Marshall, L., Johnson, F., Sharma, A., 2018. Deriving daily water levels from satellite altimetry and land surface temperature for sparsely gauged catchments: a case study for the Mekong River. *Remote Sens. Environ.* 212, 31–46.
- Portmann, F.T., Siebert, S., Döll, P., 2010. MIRCA2000—Global monthly irrigated and rainfed crop areas around the year 2000: A new high-resolution data set for agricultural and hydrological modeling. *Glob. Biogeochem. Cycles* 24.
- Qin, Q., Zhang, N., Nan, P., Chai, L., 2011. Geothermal area detection using Landsat ETM + thermal infrared data and its mechanistic analysis—a case study in Tengchong, China. *Int. J. Appl. Earth Obs. Geoinf.* 13, 552–559.
- Qin, Y., Huang, J., McVicar, T.R., West, S., Khan, M., Steven, A.D.L., 2021. Estimating surface solar irradiance from geostationary Himawari-8 over Australia: a physics-based method with calibration. *Sol. Energy* 220, 119–129.
- Qiu, J., Gao, Q., Wang, S., Su, Z., 2016. Comparison of temporal trends from multiple soil moisture data sets and precipitation: the implication of irrigation on regional soil moisture trend. *Int. J. Appl. Earth Obs. Geoinf.* 48, 17–27.
- Quarmby, N.A., Milnes, M., Hindle, T.L., Silleos, N., 1993. The use of multi-temporal NDVI measurements from AVHRR data for crop yield estimation and prediction. *Int. J. Remote Sens.* 14, 199–210.
- Rabbani, R., Zeeshan, M., 2020. Exploring the suitability of MERRA-2 reanalysis data for wind energy estimation, analysis of wind characteristics and energy potential assessment for selected sites in Pakistan. *Renew. Energy* 154, 1240–1251.
- Requejo-Castro, D., Giné-Garriga, R., Pérez-Foguet, A., 2020. Data-driven Bayesian network modelling to explore the relationships between SDG 6 and the 2030 Agenda. *Sci. Total Environ.* 710, 136014.
- Rodell, M., Houser, P.R., Jambor, U., Gottschalk, J., Mitchell, K., Meng, C.-J., Arseneault, K., Cosgrove, B., Radakovitch, J., Bosilovich, M., Entin, J.K., Walker, J.P., Lohmann, D., Toll, D., 2004. The global land data assimilation system. *Bull. Am. Meteorol. Soc.* 85, 381–394.
- Rodell, M., Velicogna, I., Famiglietti, J.S., 2009. Satellite-based estimates of groundwater depletion in India. *Nature* 460, 999–1002.
- Rodell, M., Beaudoing, H.K., L'Ecuyer, T.S., Olson, W.S., Famiglietti, J.S., Houser, P.R., Adler, R., Bosilovich, M.G., Clayton, C.A., Chambers, D., Clark, E., Fetzer, E.J., Gao, X., Gu, G., Hilburn, K., Huffman, G.J., Lettenmaier, D.P., Liu, W.T., Robertson, F.R., Schlosser, C.A., Sheffield, J., Wood, E.F., 2015. The observed state of the water cycle in the early twenty-first century. *J. Clim.* 28, 8289–8318.
- Rokni, K., Ahmad, A., Selamat, A., Hazini, S., 2014. Water feature extraction and change detection using multitemporal Landsat imagery. *Remote Sens.* 6, 4173–4189.
- Rudolf, B., Hauschild, H., Rueth, W., Schneider, U., 1994. Terrestrial precipitation analysis: operational method and required density of point measurements. *Glob. Precip. Clim. Chang.* 26.
- Rudolf, B., Becker, A., Schneider, U., Meyer-Christoffer, A., Ziese, M., 2010. The new "GPCC Full Data Reanalysis Version 5" providing high-quality gridded monthly precipitation data for the global land-surface is public available since December 2010. GPCC Status rep 7.
- Sadeghi, M., Nguyen, P., Naeini, M.R., Hsu, K., Braithwaite, D., Sorooshian, S., 2021. PERSIANN-CCS-CDR, a 3-hourly 0.04° global precipitation climate data record for heavy precipitation studies. *Sci. Data* 8, 157.
- Salmon, J.M., Friedl, M.A., Frolking, S., Wisser, D., Douglas, E.M., 2015. Global rain-fed, irrigated, and paddy croplands: a new high resolution map derived from remote sensing, crop inventories and climate data. *Int. J. Appl. Earth Obs. Geoinf.* 38, 321–334.
- Santos Da Silva, J., Calmant, S., Seyler, F., Rotunno Filho, O.C., Cochonneau, G., Mansur, W.J., 2010. Water levels in the Amazon basin derived from the ERS 2 and ENVISAT radar altimetry missions. *Remote Sens. Environ.* 114, 2160–2181.
- Sarp, G., Ozcelik, M., 2017. Water body extraction and change detection using time series: A case study of Lake Burdur, Turkey. *J. Taibah Univ. Sci.* 11, 381–391.
- Schamm, K., Ziese, M., Becker, A., Finger, P., Meyer-Christoffer, A., Schneider, U., Schröder, M., Stender, P., 2014. Global gridded precipitation over land: a description of the new GPCC First Guess Daily product. *Earth Syst. Sci. Data* 6, 49–60.
- Scharlemann, J.P.W., Brock, R.C., Balfour, N., Brown, C., Burgess, N.D., Guth, M.K., Ingram, D.J., Lane, R., Martin, J.G.C., Wicander, S., Kapos, V., 2020. Towards understanding interactions between Sustainable Development Goals: the role of environment-human linkages. *Sustain. Sci.* 15, 1573–1584.
- Schwatke, C., Dettmering, D., Bosch, W., Seitz, F., 2015. DAHITI – an innovative approach for estimating water level time series over inland waters using multi-mission satellite altimetry. *Hydrol. Earth Syst. Sci.* 19, 4345–4364.
- Senay, G.B., Kagine, S., Velpuri, N.M., 2020. Operational global actual evapotranspiration: development, evaluation, and dissemination. *Sensors* 20, 1915.
- Sengupta, M., Xie, Y., Lopez, A., Habte, A., Maclaurin, G., Shelby, J., 2018. The National Solar Radiation Data Base (NSRDB). *Renew. Sust. Energ. Rev.* 89, 51–60.
- Shen, Y., Liu, D., Jiang, L., Nielsen, K., Yin, J., Liu, J., Bauer-Gottwein, P., 2022. High-resolution water level and storage variation datasets for 338 reservoirs in China during 2010–2021. *Earth Syst. Sci. Data* 14, 5671–5694.
- Shi, Y., Ji, S.-P., Shao, X.-W., Tang, H.-J., Wu, W.-B., Yang, P., Zhang, Y.-J., Ryosuke, S., 2014. Framework of SAGI agriculture remote sensing and its perspectives in supporting national food security. *J. Integr. Agric.* 13, 1443–1450.
- Shi, S., Ye, Y., Xiao, R., 2022. Evaluation of food security based on remote sensing data—taking Egypt as an example. *Remote Sens.* 14, 2876.
- Siebert, S., Burke, J., Faures, J.M., Frenken, K., Hoogeveen, J., Döll, P., Portmann, F.T., 2010. Groundwater use for irrigation – a global inventory. *Hydrol. Earth Syst. Sci.* 14, 1863–1880.
- Siebert, S., Henrich, V., Frenken, K., Burke, J., 2013. Update of the digital global map of irrigation areas to version 5. *Rheinische Friedrich-Wilhelms-Universität, Bonn, Germany and Food and Agriculture Organization of the United Nations, Rome, Italy.*

- Singh, A., Seitz, F., Schwatke, C., 2012. Inter-annual water storage changes in the Aral Sea from multi-mission satellite altimetry, optical remote sensing, and GRACE satellite gravimetry. *Remote Sens. Environ.* 123, 187–195.
- Sitterson, J., Knights, C., Parmar, R., Wolfe, K., Avant, B., Muche, M., 2018. An overview of rainfall-runoff model types.
- Skofronick-Jackson, G., Hudak, D., Petersen, W., Nesbitt, S.W., Chandrasekar, V., Durden, S., Gleicher, K.J., Huang, G.-J., Joe, P., Kollias, P., Reed, K.A., Schwaller, M.R., Stewart, R., Tanelli, S., Tokay, A., Wang, J.R., Wolde, M., 2015. Global Precipitation Measurement Cold Season Precipitation Experiment (GCPEX) For measurement's sake, let it snow. *Bull. Am. Meteorol. Soc.* 96, 1719–1742.
- Skriver, H., Mattia, F., Satalino, G., Balenzano, A., Pauwels, V.R.N., Verhoest, N.E.C., Davidson, M., 2011. Crop classification using short-revisit multitemporal SAR data. *IEEE J. Select. Top. Appl. Earth Observ. Remote Sens.* 4, 423–431.
- Smith, L.C., 1997. Satellite remote sensing of river inundation area, stage, and discharge: a review. *Hydrol. Process.* 11, 1427–1439.
- Sorooshian, S., Nguyen, P., Sellars, S., Braithwaite, D., Aghakouchak, A., Hsu, K., 2014. Satellite-based remote sensing estimation of precipitation for early warning systems. In: Ismail-Zadeh, A., Kijko, A., Zaliapin, I., Urrutia Fucugauchi, J., Takeuchi, K. (Eds.), *Extreme Natural Hazards, Disaster Risks and Societal Implications*. Cambridge University Press, Cambridge.
- Spennemann, P.C., Rivera, J.A., Saulo, A.C., Penalba, O.C., 2015. A Comparison of GLDAS Soil Moisture Anomalies against Standardized Precipitation Index and Multisatellite Estimations over South America. *J. Hydrometeorol.* 16, 158–171.
- Srivastava, P.K., Bhattacharya, A.K., 2006. Groundwater assessment through an integrated approach using remote sensing, GIS and resistivity techniques: a case study from a hard rock terrain. *Int. J. Remote Sens.* 27, 4599–4620.
- Staffell, I., Pfenninger, S., 2016. Using bias-corrected reanalysis to simulate current and future wind power output. *Energy* 114, 1224–1239.
- Steere-Dunne, S.C., McNairn, H., Monsivais-Huertero, A., Judge, J., Liu, P.W., Papathanassiou, K., 2017. Radar remote sensing of agricultural canopies: a review. *IEEE J. Select. Top. Appl. Earth Observ. Remote Sens.* 10, 2249–2273.
- Sulistioadi, Y.B., Tseng, K.H., Shum, C.K., Hidayat, H., Sumaryono, M., Suhardiman, A., Setiawan, F., Sunarso, S., 2015. Satellite radar altimetry for monitoring small rivers and lakes in Indonesia. *Hydrol. Earth Syst. Sci.* 19, 341–359.
- Sun, W., Ishidaira, H., Bastola, S., Yu, J., 2015. Estimating daily time series of streamflow using hydrological model calibrated based on satellite observations of river water surface width: toward real world applications. *Environ. Res.* 139, 36–45.
- Sun, Q., Miao, C., Duan, Q., Ashouri, H., Sorooshian, S., Hsu, K.-L., 2018. A review of global precipitation data sets: data sources, estimation, and intercomparisons. *Rev. Geophys.* 56, 79–107.
- Susnik, J., Masia, S., Indrikstone, D., Brémere, I., Vamvakleridou-Lydroudia, L., 2021. System dynamics modelling to explore the impacts of policies on the water-energy-food-land-climate nexus in Latvia. *Sci. Total Environ.* 775, 145827.
- Tang, G., Clark, M.P., Papalexiou, S.M., Ma, Z., Hong, Y., 2020. Have satellite precipitation products improved over last two decades? A comprehensive comparison of GPM IMERG with nine satellite and reanalysis datasets. *Remote Sens. Environ.* 240, 111697.
- Teluguntla, P., Thenkabail, P., Oliphant, A., Gumma, M., Aneece, I., Foley, D., McCormick, R., 2023. Landsat-Derived Global Rainfed and Irrigated-Cropland Product 30 m V001. In: DAAC, N. E. L. P. (ed.).
- The Global Runoff Data Centre, 2020. 56068 Koblenz. Germany.
- Thenkabail, P.S., Biradar, C.M., Noojipady, P., Dheeravath, V., Li, Y., Velpuri, M., Gumma, M., Gangalakunta, O.R.P., Tural, H., Cai, X., Vithanage, J., Schull, M.A., Dutta, R., 2009. Global irrigated area map (GIAM), derived from remote sensing, for the end of the last millennium. *Int. J. Remote Sens.* 30, 3679–3733.
- Thenkabail, P.S., Hanjra, M.A., Dheeravath, V., Gumma, M., 2010. A holistic view of global croplands and their water use for ensuring global food security in the 21st century through advanced remote sensing and non-remote sensing approaches. *Remote Sens.* 2, 211–261.
- Thenkabail, P.S., Teluguntla, P.G., Xiong, J., Oliphant, A., Congalton, R.G., Ozdogan, M., Gumma, M.K., Tilton, J.C., Giri, C., Milesi, C., Phalke, A., Massey, R., Yadav, K., Sankey, T., Zhong, Y., Aneece, I., Foley, D., 2021. Global cropland-extent product at 30-m resolution (GCEP30) derived from Landsat satellite time-series data for the year 2015 using multiple machine-learning algorithms on Google Earth Engine cloud. Professional Paper, Reston, VA.
- Tilman, D., Balzer, C., Hill, J., Befort, B.L., 2011. Global food demand and the sustainable intensification of agriculture. *Proc. Natl. Acad. Sci.* 108, 20260–20264.
- Treichler, D., Käab, A., 2017. Snow depth from ICESat laser altimetry — a test study in southern Norway. *Remote Sens. Environ.* 191, 389–401.
- UNECE, 2015. Reconciling Resource Uses in Transboundary Basins: Assessment of the Water-Food-Energy-Ecosystems Nexus. Geneva, Switzerland.
- UNFCCC, 2022. *Nationally Determined Contributions (NDCs)* [Online]. Available: <http://unfccc.int/process-and-meetings/the-paris-agreement/nationally-determined-contributions-ndcs> [Accessed 07 April 2022].
- United Nations, 2021. *Goal 7: Ensure access to affordable, reliable, sustainable and modern energy for all* [Online]. Available: <https://sdgs.un.org/goals/goal7> [Accessed 20 July 2021].
- USGS, 2018. *Digital Elevation - Shuttle Radar Topography Mission (SRTM) 1 Arc-Second Global* [Online]. usgs.gov. Available: <https://www.usgs.gov/centers/eros/science/usgs-eros-archive/digital-elevation-shuttle-radar-topography-mission-srtm-1> [Accessed 24 March 2022].
- Van Der Meer, F., Hecker, C., Van Ruitenbeek, F., Van Der Werff, H., De Wijkerslooth, C., Wechsler, C., 2014. Geologic remote sensing for geothermal exploration: A review. *Int. J. Appl. Earth Obs. Geoinf.* 33, 255–269.
- Van Dijk, A.I.J.M., Brakenridge, G.R., Kettner, A.J., Beck, H.E., De Groot, T., Schellekens, J., 2016. River gauging at global scale using optical and passive microwave remote sensing. *Water Resour. Res.* 52, 6404–6418.
- Vaughan, R.G., Keszthelyi, L.P., Lowenstein, J.B., Jaworowski, C., Heasler, H., 2012. Use of ASTER and MODIS thermal infrared data to quantify heat flow and hydrothermal change at Yellowstone National Park. *J. Volcanol. Geotherm. Res.* 233, 72–89.
- Viña, A., Gitelson, A.A., Ngui-Robertson, A.L., Peng, Y., 2011. Comparison of different vegetation indices for the remote assessment of green leaf area index of crops. *Remote Sens. Environ.* 115, 3468–3478.
- Vinca, A., Parkinson, S., Riahi, K., Byers, E., Siddiqi, A., Muhammad, A., Ilyas, A., Yugeswaran, N., Willaarts, B., Magnuszewski, P., Awais, M., Rowe, A., Djilali, N., 2021a. Transboundary cooperation a potential route to sustainable development in the Indus basin. *Nat. Sustain.* 4, 331–339.
- Vinca, A., Riahi, K., Rowe, A., Djilali, N.J.E.S., 2021b. Climate-land-energy-water nexus models across scales: progress, gaps and best accessibility practices. *Front.* 9, 691523.
- Vindel, J.M., Navarro, A.A., Valenzuela, R.X., Ramírez, L., 2016. Temporal scaling analysis of irradiance estimated from daily satellite data and numerical modelling. *Atmos. Res.* 181, 154–162.
- Waewsaik, J., Chancham, C., Chiwamongkhonkarn, S., Gagnon, Y., 2019. Wind resource assessment of the southernmost region of Thailand using atmospheric and computational fluid dynamics wind flow modeling. *Energies* 12, 1899.
- Wagner, W., Hahn, S., Kidd, R., Melzer, T., Bartalis, Z., Hasenauer, S., Figa, J., De Rosnay, P., Jann, A., Schneider, S., 2013. The ASCAT soil moisture product: a review of its. *Meteorol. Z.* 22, 1–29.
- Wang, X., Xie, H., 2018. A Review on Applications of Remote Sensing and Geographic Information Systems (GIS) in Water Resources and Flood Risk Management. *Water* 10, 608.
- Wang, J., Walter, B.A., Yao, F., Song, C., Ding, M., Maroof, A.S., Zhu, J., Fan, C., McAlister, J.M., Sikder, S., Sheng, Y., Allen, G.H., Crétaux, J.F., Wada, Y., 2022. GeoDAR: georeferenced global dams and reservoirs dataset for bridging attributes and geolocations. *Earth Syst. Sci. Data* 14, 1869–1899.
- Weber, M., Koch, F., Bernhardt, M., Schulz, K., 2021. The evaluation of the potential of global data products for snow hydrological modelling in ungauged high-alpine catchments. *Hydrol. Earth Syst. Sci.* 25, 2869–2894.
- Wei, X., Duan, Y., Liu, Y., Jin, S., Sun, C., 2019. Onshore-offshore wind energy resource evaluation based on synergistic use of multiple satellite data and meteorological stations in Jiangsu Province, China. *Front. Earth Sci.* 13, 132–150.
- Western Geographic Science Center, 2018. *Global Food Security-Support Analysis Data at 30 m (GFSAD)* [Online]. USGS. Available: [https://www.usgs.gov/gov/centers/western-geograph/ic-science-center/science/global-food-security-support-analysis-data-30-m?qt-science\\_center\\_objects=3#overview](https://www.usgs.gov/gov/centers/western-geograph/ic-science-center/science/global-food-security-support-analysis-data-30-m?qt-science_center_objects=3#overview) [Accessed 05 January 2023].
- Wicaksono, A., Jeong, G., Kang, D., 2017. Water, energy, and food nexus: review of global implementation and simulation model development. *Water Policy* 19, 440–462.
- WMO, 2008. *Guide to Hydrological Practice: Volume I: Hydrology – From Measurement to Hydrological Information*. World Meteorological Organization.
- World Economic Forum, 2011. Water security: the water-food-energy-climate nexus: the World Economic Forum water initiative. Washington.
- Wrzesien, M.L., Pavelsky, T.M., Durand, M.T., Dozier, J., Lundquist, J.D., 2019. Characterizing biases in mountain snow accumulation from global data sets. *Water Resour. Res.* 55, 9873–9891.
- Wu, C., Wang, L., Niu, Z., Gao, S., Wu, M., 2010. Nondestructive estimation of canopy chlorophyll content using Hyperion and Landsat/TM images. *Int. J. Remote Sens.* 31, 2159–2167.
- Xiang, Y., Chen, J., Li, L., Peng, T., Yin, Z., 2021. Evaluation of eight global precipitation datasets in hydrological modeling. *Remote Sens.* 13, 2831.
- Xiao, X., Boles, S., Liu, J., Zhuang, D., Frolking, S., Li, C., Salas, W., Moore, B., 2005. Mapping paddy rice agriculture in southern China using multi-temporal MODIS images. *Remote Sens. Environ.* 95, 480–492.
- Xie, P., Chen, M., Shi, W., 2010. CPC unified gauge-based analysis of global daily precipitation. *Preprints, 24th Conf. on Hydrology*, Atlanta, GA, Amer. Meteor. Soc.
- Xie, P., Joyce, R., Wu, S., Yoo, S., Yarosh, Y., Sun, F., Lin, R., 2019. NOAA Climate Data Record (CDR) of CPC Morphing Technique (CMORPH) High Resolution Global Precipitation Estimates. Version.
- Xie, Y., Gibbs, H.K., Lark, T.J., 2021. Landsat-based Irrigation Dataset (LANID): 30 m resolution maps of irrigation distribution, frequency, and change for the US, 1997–2017. *Earth Syst. Sci. Data* 13, 5689–5710.
- Xu, H., 2006. Modification of normalised difference water index (NDWI) to enhance open water features in remotely sensed imagery. *Int. J. Remote Sens.* 27, 3025–3033.
- Xu, N., Zheng, H., Ma, Y., Yang, J., Liu, X., Wang, X., 2021. Global estimation and assessment of monthly lake/reservoir water level changes using ICESat-2 ATL13 products. *Remote Sens.* 13, 2744.
- Yamazaki, D., Ikeshima, D., Sosa, J., Bates, P.D., Allen, G.H., Pavelsky, T.M., 2019. MERIT hydro: a high-resolution global hydrography map based on latest topography dataset. *Water Resour. Res.* 55, 5053–5073.
- Yang, Y.C.E., Ringler, C., Brown, C., Mondal, M.A.H., 2016. Modeling the Agricultural Water-Energy-Food Nexus in the Indus River Basin, Pakistan, 142, 04016062.
- Yang, J., Yang, Y.C.E., Khan, H.F., Xie, H., Ringler, C., Ogilvie, A., Seidou, O., Djibo, A.G., Weert, V.A.N., F., & Tharme, R., 2018. Quantifying the Sustainability of Water Availability for the Water-Food-Energy-Ecosystem Nexus in the Niger River Basin, 6, pp. 1292–1310.
- Yang, P., Van Der Tol, C., Verhoef, W., Damm, A., Schickling, A., Kraska, T., Muller, O., Rascher, U., 2019. Using reflectance to explain vegetation biochemical and

- structural effects on sun-induced chlorophyll fluorescence. *Remote Sens. Environ.* 231, 110996.
- Yeh, P.J.F., Swenson, S.C., Famiglietti, J.S., Rodell, M., 2006. Remote sensing of groundwater storage changes in Illinois using the Gravity Recovery and Climate Experiment (GRACE). *Water Resour. Res.* 42.
- Young, I.R., Kirezci, E., Ribal, A., 2020. The global wind resource observed by scatterometer. *Remote Sens.* 12, 2920.
- Yu, Y., Shi, J., Wang, T., Letu, H., Yuan, P., Zhou, W., Hu, L., 2019. Evaluation of the Himawari-8 Shortwave Downward Radiation (SWDR) product and its comparison with the CERES-SYN, MERRA-2, and ERA-interim datasets. *IEEE J. Select. Top. Appl. Earth Observ. Remote Sens.* 12, 519–532.
- Yuan, C., Gong, P., Bai, Y., 2020. Performance assessment of ICESat-2 laser altimeter data for water-level measurement over lakes and reservoirs in China. *Remote Sens.* 12, 770.
- Zanaga, D., Van De Kerchove, R., Daems, D., De Keersmaecker, W., Brockmann, C., Kirches, G., Wevers, J., Cartus, O., Santoro, M., Fritz, S., 2022. ESA WorldCover 10 m 2021 v200.
- Zhang, K., Kimball, J.S., Nemani, R.R., Running, S.W., 2010. A continuous satellite-derived global record of land surface evapotranspiration from 1983 to 2006. *Water Resour. Res.* 46.
- Zhang, K., Kimball, J.S., Running, S.W., 2016a. A review of remote sensing based actual evapotranspiration estimation. *WIREs Water* 3, 834–853.
- Zhang, X., Liang, S., Wang, G., Yao, Y., Jiang, B., Cheng, J., 2016b. Evaluation of the Reanalysis Surface Incident Shortwave Radiation Products from NCEP, ECMWF, GSFC, and JMA Using Satellite and Surface Observations. *Remote Sens.* 8, 225.
- Zhang, C., Chen, X., Li, Y., Ding, W., Fu, G., 2018. Water-energy-food nexus: concepts, questions and methodologies. *J. Clean. Prod.* 195, 625–639.
- Zhang, Y., Kong, D., Gan, R., Chiew, F.H.S., McVicar, T.R., Zhang, Q., Yang, Y., 2019. Coupled estimation of 500 m and 8-day resolution global evapotranspiration and gross primary production in 2002–2017. *Remote Sens. Environ.* 222, 165–182.
- Zhao, G., Gao, H., 2018. Automatic correction of contaminated images for assessment of reservoir surface area dynamics. *Geophys. Res. Lett.* 45, 6092–6099.
- Zhao, L., Lee, X., Liu, S., 2013. Correcting surface solar radiation of two data assimilation systems against FLUXNET observations in North America. *J. Geophys. Res.-Atmos.* 118, 9552–9564.
- Zhou, Y., Wu, W.X., Liu, G.X., 2011. Assessment of onshore wind energy resource and wind-generated electricity potential in Jiangsu, China. *Energy Procedia* 5, 418–422.
- Zreda, M., Shuttleworth, W., Zeng, X., Zweck, C., Desilets, D., Franz, T., Rosolem, R., 2012. COSMOS: the cosmic-ray soil moisture observing system. *Hydrol. Earth Syst. Sci.* 16, 4079–4099.